Alma Mater Studiorum – Università di Bologna

DOTTORATO DI RICERCA IN

Scienze Veterinarie

Ciclo XXXII

Settore Concorsuale: 07/H2 – PATOLOGIA VETERINARIA E ISPEZIONE DEGLI ALIMENTI DI ORIGINE ANIMALE

Settore Scientifico Disciplinare: VET03 - PATOLOGIA GENERALE E ANATOMIA PATOLOGICA VETERINARIA

Melanoma maligno orale canino: approccio genomico e immunoistochimico per meglio caratterizzare la disseminazione metastatica al linfonodo

Presentata da: Dr. Stefano Di Palma

Coordinatore Dottorato **Supervisore**

Prof. Arcangelo Gentile **Prof. Barbara Brunetti**

Esame finale anno 2020

Alma Mater Studiorum – Università di Bologna

DOCTORAL PROGRAM IN

Veterinary Science

XXXII Cycle

Academic Recruitment Field: 07/H2 – VETERINARY PATHOLOGY AND INSPECTION OF FOOD OF ANIMAL ORIGIN

Scientific Section: VET03 – GENERAL PATHOLOGY AND VETERINARY ANATOMIC PATHOLOGY

Canine oral malignant melanoma: genomic and immunohistochemical approaches to better characterize the metastatic dissemination to the lymph node

PhD Candidate: Dr. Stefano Di Palma

PhD Program Coordinator: **Prof. Arcangelo Gentile**

PhD Candidate Supervisor: **Prof. Barbara Brunetti**

Final exam 2020

Table of Contents

Abstract **8**

Introduction **10**

Origin and functions of melanocytes 10

Canine oral malignant melanoma and its role as a model for human disease 10

The clinical relevance of the regional/draining lymph node metastases 13

Metastatic dissemination as a sign of malignant transformation 14

Malignant melanoma genomics 16

Aims **19**

Chapter 1: Gene expression profiling of canine primary OMMs and their lymph node metastases **21**

Materials and methods **23**

Ethics Statements 23

Tumour Samples 23

RNA isolation, purification and quantification 24

Global gene expression profiling 25

Results **27**

Purity and quantity of total RNA isolated from FFPE OMM biopsies 27

Tumours included in differential expression analysis 30

Genes displaying differential expression between primary and metastatic OMMs 30

Functional annotation enrichment analysis 33

Discussion **34**

Cell motility 34

Cell interactions 41

Cancer progression and cell survival 43

Conclusions 45

Limitations of the study 46

Future work 47

Chapter 2: Lymphatic invasion in canine oral melanoma: can the sensitivity of detection be increased by Prox-1 immunohistochemical staining for lymphatic endothelial cells? **49**

Materials and methods **51**

Ethics Statements 51

Tumour Samples 51

Evaluation of lymphatic invasion 51
Statistical analysis 53
Results 54
Interobserver agreement on lymphatic invasion in canine primary OMMs 54
Sensitivity and specificity of detection of lymphatic invasion in predicting lymph nodal metastasis 60
Discussion 63
Limitations of the study 66
Future work 66
Scientific activity carried out during the PhD 69
Appendix 1 74
Appendix 2 76
Appendix 3 77
Appendix 4 78
Appendix 5 79
Appendix 6 85
Acknowledgment 88
Bibliography 90

Abstract:

Malignant melanoma is the most common malignant tumour of the oral cavity in the dog, with high rate of metastatic dissemination to the regional lymph nodes and distant organs. There is significant overlap in regards of biologic behaviour, histological appearance and genomic alterations between canine and human OMMs. Therefore, the dog is considered a good preclinical model for this deadly tumour.

In the first part of this study we aimed to identify genes that are involved in the metastatic dissemination of canine OMMs by microarray mRNA profiling of 4 pairs of primary tumours and their lymph nodal metastases. These genes could represent a future target for the control and hopefully treatment of the metastatic disease. We pointed out the presence of several genes displaying different expression between the primary and the metastatic tumour. In particular, Rac1 seems to play a key role in the dissemination of melanoma cells to the lymph node, most likely due to its regulatory activity of cell motility.

In the second part of the study we assessed the potential improvement of detection of lymphatic invasion in canine primary OMMs by using immunohistochemistry for Prox-1, as the detection of lymphatic invasion in a primary tumour is generally considered an unfavourable prognostic factor for several cancers, including human and canine OMMs. We also tried to prove direct correlation between the presence of lymphatic invasion in the primary tumour and regional lymph node metastasis. Our results showed that Prox-1 IHC is not able to enhance detection of lymphatic invasion in the primary site and that the sensitivity of detection of lymphatic invasion in predicting lymph nodal metastasis is low (46.7%), despite high specificity (97%). Finally, we pointed out the presence of interobserver variability in detecting lymphatic invasion in canine primary OMMs, most likely due to interpretative variation.

Introduction:

Origin and functions of melanocytes:

In vertebrates, melanocytic stem cells originate from the neural crest, emigrate dorsolaterally from the neural tube and reach the skin and mucous membranes during embryonal development. In the epidermis these stem cells reside in the bulge region of the hair follicle although the specific niche in which they reside in the oral mucosa is still unknown. As mature melanocytes, they localize in the basal cell layer of the epithelium. They are stellate/dendritic cells able to disseminate membrane-bound organelles containing melanin (called melanosomes) to the keratinocytes via a network of arborizing processes (dendrites). Melanosomes can contain variable amounts of eumelanin (imparting a dark colour) and pheomelanin (associated with light skin). Different sized melanosomes containing different proportions of eumelanin and pheomelanin will determine all the skin/mucosa colour variations [1].

Melanin synthesis (confined only to melanocytes and retinal pigment cells) is catalysed by the enzyme tyrosinase, which converts tyrosine to dihydroxyphenylalanine (DOPA)[2]. The lack of this enzyme results in albinism. Once transported to the keratinocytes, the melanin pigment is mainly located over the nucleus forming a supranuclear "cap" in order to protect the nuclear DNA from ultraviolet (UV) damage [3]. Melanin is not only involved in protection against UV damage and imparting colour of skin/mucosal surfaces but has several other functions. For example, this pigment is able to provide protection against reactive oxygen species (ROS) and free radicals, neutralize bacterial enzymes and toxins, and act like a physical barrier against microorganisms. Melanocytes have several other functions apart from the synthesis of melanin. Indeed, they can be involved in the immune response, mainly as part of the innate immune system. They can act like antigen-presenting cells, stimulate T-cell proliferation and show phagocytic activity against microorganisms [4].

Canine oral malignant melanoma and its role as a model for human disease:

Incidence:

Oral cancer accounts for 6% to 7% of canine cancers and malignant melanoma is the most common cancer of the oral cavity in dogs (30-40% of oral malignancies)[5,6].

Overrepresented breeds are the Cocker Spaniel, Miniature Poodle, Anatolian Sheepdog, Gordon Setter, Chow Chow, and Golden Retriever[5].

In human medicine, oral melanomas are considered part of the larger group of mucosal melanomas together with melanomas arising from the anogenital regions, oropharynx, paranasal sinuses, conjunctiva, parotid glands, oesophagus and the middle ear. They represent a rare clinical entity (with a reported incidence of 800 cases per year in the United States, in contrast to cutaneous melanomas which are 100x more common)[7].

The incidence reported in the literature points out racial differences with Asians having a higher incidence of head and neck mucosal melanomas. Intriguingly, in Japan oral mucosal melanoma accounts for 7.5% of all melanomas, in contrast with 1% of all melanomas in Caucasians[8].

Biologic behaviour:

In general, canine oral malignant melanomas (OMMs) show more aggressive biologic behaviour and shorter median survival time compared to their cutaneous counterpart. For dogs treated with surgery alone, the survival rate is less than 35% and metastases to regional lymph nodes and distant organs are frequently reported (in up to 74% of cases)[6,5].

Human OMMs carry a poor prognosis with a 5-year survival rate of between 25 and 33% according to the disease stage and location. Head and neck mucosal melanomas present with local and/or distant metastasis to the lungs and liver in 50% of cases. Lymph node metastatic dissemination is reported in 33% of OMM patients[9,7].

Histopathology:

Several histologic variants of oral melanoma are recognized in the dog: epithelioid, spindloid/fibromatous, mixed, and rare types such as whorled/dendritic, balloon cell, signet ring cell, clear cell and adenoid/papillary cell[6]. Amelanotic melanomas represent approximately 30% of all canine melanoma cases[10].

Common growth patterns found in human mucosal melanomas are spindled, perivascular/peritheliomatous, and solid, with other less-commonly encountered

patterns (pseudopapillary, storiform, and alveolar). Head and neck mucosal melanomas are frequently amelanotic (up to 50% of tumours)[7].

Somatic mutation profiles:

Similarities between the somatic profiles of human mucosal melanomas and canine OMMs have been identified. Mutations in NRAS have been described in canine OMMs at the same hotspots ($NRAS^{Q61}$) as in human cancers. In humans, $NRAS^{Q61}$ is the most frequent somatic alteration found in NRAS-mutated melanomas, and in mice models this mutation is known to interact with INK4A or β-catenin mutations to promote melanoma[11]. Canine OMMs presents numerous copy number alterations and a relatively low single nucleotide variation rate with general non-UV mutation signatures, as showed in human mucosal melanomas[9]. The "chromothripsis like" profile on CFA30 has been reported in canine OMMs and corresponds to the HSA15 alteration observed in human cases. In both species, the MAPK and PI3K pathways are both involved in OMM formation and progression[9]. Interestingly, a recent study has focused on presence of recurrently mutated driver genes in different species, comparing mucosal human, oral canine and mucosal-like/mucocutaneous equine melanomas. In this study, NRAS and TP53 were mutated and PTEN was disrupted by nonsense or frameshift mutations in all 3 species[12].

Conclusion:

Dogs represent a relevant preclinical model for human OMMs as naturally occurring canine OMMs share several clinical and histopathological characteristics as well as somatic mutation profiles with the human disease[13]. The major benefits of dogs as tumour models include the ability to study animals in which cancers develop spontaneously and thus are more like reflect the process of human tumourigenesis compared to experimentally-induced neoplasms. Furthermore, pets and owners share the same environment and they may be exposed to the same carcinogens, which can contribute to the tumour development[9].

The clinical relevance of the regional/draining lymph node metastases:

Lymphatic vessels are built for transport of fluid and cells away from tissues and therefore it may not be surprising that this system represents a major route for dissemination of tumour cells. Presence of lymphovascular invasion (LVI) in a primary tumour (defined as tumour emboli present within a definite endothelial-lined space) is generally considered an unfavourable prognostic factor and has been shown to be an independent predictor of worse survival in several human cancers[14–17]. Presence of LVI has also been associated with the decreased overall survival of dogs with melanocytic tumours[18]. However, reported incidence of LVI is disproportionately low compared to the incidence of sentinel lymph node positivity on routine histologic evaluation in humans[19]. Several factors may contribute to the low rate of definitive LVI such as misinterpretation of stromal retraction artefacts and difficulties with identifying lymphatic emboli when tumour cells completely fill the lumen.

Immunohistochemistry using antibodies specific to the lymphatic endothelium such as lymphatic vessel endothelial hyaluronan receptor 1 (LYVE-1) and D2-40 (detecting an epitope on podoplanin) has been used in several studies on human cutaneous melanomas to assess the potential increased detection of lymphatic invasion compared to routine haematoxylin and eosin (H&E) staining. It has been shown that this technique is able to enhance the detection of lymphatic invasion up to nine folds compared to H&E staining[20].

In veterinary medicine, Sleeckx et al[21] tried to assess different specific lymphatic endothelial markers in canine FFPE mammary tissue. In this study D2-40 did not show immunoreactivity with FFPE canine tissue. Anti-prospero-related homeobox I (Prox-1) antibody was considered the best antibody compared to LYVE-1 due to stronger positive signal and lower background. However, to our knowledge Prox-1 has been only used in canine FFPE tissue to evaluate the intestinal lymphatic vasculature[22], to differentiate cutaneous angiosarcoma[23] and to assess lymphangiogenesis in mammary tumours[24] but never to enhance detection of LVI.

After entering the lymphatic system in the primary tumour, neoplastic cells start their journey to the regional/sentinel lymph node. The survival and growth of neoplastic cells in the metastatic site is strictly related to interactions between the “seed” (cancer cells) and “soil” (microenvironment). These interactions have been shown to involve chemokine receptors on cancer cells and their ligands in the target organs. Interestingly, CXCR3, CXCR4 and CCR7 play a critical role in lymph node metastasis

in several human cancers[25]. In particular, CCR7 is able to dramatically increase metastasis to a draining lymph node when expressed in B16 murine melanoma cells[26] and suppression of CXCR3 expression in B16F10 murine melanoma cells reduces the metastatic frequency of these cells to the draining lymph nodes[27].

Lymphatic invasion, and in particular regional/draining lymph node metastases, are considered an important prognostic factor in many types of human cancer including oral melanomas[8], being associated with a poorer prognosis and partially dictating the course of treatment[28]. Additional studies are needed in order to make definitive conclusions regarding the clinical significance of lymph node metastasis for canine OMMs[29]. Indeed, only few studies have specifically examined regional lymph node metastasis as a prognostic factor, despite local lymph node aspiration with cytology being part of the routine staging process for canine OMMs[5].

Despite being recognized as an important prognostic indicator, in human medicine there is still an ongoing debate about the role of lymph node metastasis in the progression of the disease. Lymph node metastases are indeed considered clinically inconsequential by some experts, although others consider them to have the potential to seed distant organs. Recently it has been showed by Pereira et al.[28] that in a melanoma mouse model all animals had lung metastases that originated from both lymph node lesions and directly from the primary tumour. Additionally, they revealed that lymph node metastases most likely disseminate by invasion of lymph node blood vessels rather than through efferent lymphatic vessels. Therefore, although the route of cancer dissemination is complex and highly debated, lymph node metastases can be a source of cancer cells for distant metastases. Further studies are needed to clarify the role of the local dissemination to the regional/draining lymph node in the progression of the disease.

Metastatic dissemination as a sign of malignant transformation:

Eight alterations of normal cell physiology have been identified in the vast majority of malignant neoplastic cells as essential to determine a malignant phenotype: (1) self-sufficiency in growth signals, (2) insensitivity to anti-growth signals, (3) altered cellular metabolism, (4) ability to evade apoptosis, (5) limitless replicative potential, (6) sustained angiogenesis, (7) tissue invasion and metastasis, and (8) evasion of the host immune response[30].

The development of malignant melanocytic neoplasms is attributed to a combination of environmental factors and genetic predisposition. Unfortunately, while increased UV light exposure is a well-known environmental risk factor for human cutaneous melanomas, unknown factors contribute to oral melanoma tumorigenesis[31,32].

Tissue invasion and metastasis are biological hallmarks of malignant tumours as benign tumours do not metastasise. Metastasis is defined by the spread of neoplastic cells to sites physically discontinuous with the primary tumour. They can reach these sites by penetration into blood vessels, lymphatics, and body cavities[30].

Metastatic dissemination appears to be facilitated by pro-metastatic genetic and epigenetic changes to the primary tumour genome, and interactions between tumour cells and other cells in both the initial and distant microenvironments. Identification of pro-metastatic genetic and epigenetic events, and characterization of the pathways underpinning the metastatic cascade, is critical to discover molecular targets for the prevention and treatment of distant metastases, as this process accounts for the largest numbers of deaths from cancer. Metastatic dissemination is complex and inefficient: neoplastic cells able to metastasise are rare clones in primary tumours, with 0.01% or fewer cancer cells entering the circulation and developing into metastases[33].

In malignant melanomas, neoplastic cells are able to disseminate to distant sites most likely due to their plastic and highly migratory behaviour that resembles that of neural crest cells (NCCs), their embryonic precursors. The malignant neoplastic cells, unlikely NCCs, reactivate pro-migratory and pro-invasive pathways resulting in aberrant dissemination[34].

Cell migration is a key function of life, establishing and maintaining the proper organization in unicellular and multicellular organisms. Large scale migration of epithelial sheets during gastrulation or movement of individual cells in the nervous system are vital for the development of complex organisms. Later in life, cell migration is critical for proper immune response, wound repair, and tissue homeostasis[35]. This process is almost exclusively based on dynamic assembly and disassembly of actin filaments. Protrusion of the plasma membrane is mainly formed at the migrating front edge of cells and initiate the process of migration[36]. One mechanism to achieve this protrusion is the generation of Arp2/3 complex-containing network, such as the lamellopodium. Lamellipodia are formed at the cell periphery by continuous branching of the Arp2/3 complex and are frequently associated with mesenchymal migration[37].

Comparable structures involving Arp2/3 complex-dependent actin remodelling include podosomes and invadopodia[38]. Podosomes and invadopodia are called "invadosomes". They are adhesion and invasion structures that establish contact with the extracellular matrix (EM) and recruit metalloprotease to degrade it[39]. Podosomes reflect the physiological aspect of these structures and are formed in several normal cells, including neural crest cells[40], whereas invadopodia are found in cancer cells, such as melanoma cells[41].

Rho GTPases family is a key regulator factor in both lamellipodia and invasosomes formation. In particular, lamellipodia require the activity of the Arp2/3 complex, which is activated downstream of the Rac subfamily of small GTPases targeting WAVE regulatory complex. On the other hand, invasosomes formation depends on WASP-mediated activation of the Arp2/3 complex by Cdc42[39].

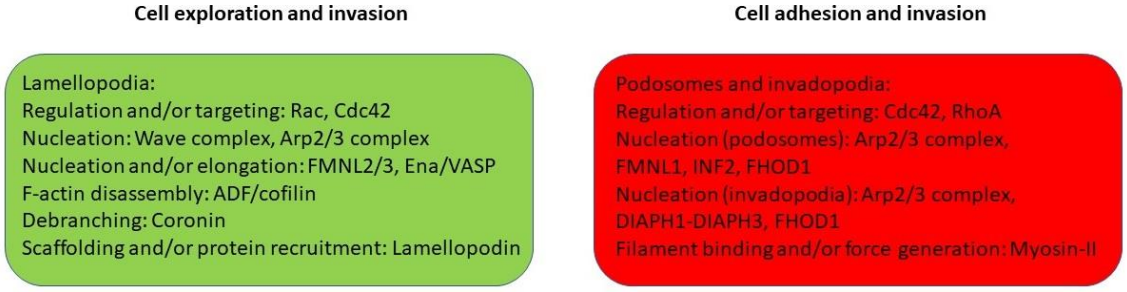

Recent studies have focused on some of the key players in cytoskeletal organization and cell migration, such as RAC1, Fascin1, Lamellipodin and the Scar/WAVE complex, to better understand the normal melanoblast behaviour during embryonal migration and proliferation[42–44] and their potential role in the metastatic process.

Malignant melanoma genomics:

Several studies have been conducted in human medicine to try to identify biomarkers for melanoma progression and metastasis by use of "omics" platforms such as genomics, proteomics, microRNA and exosome analysis.

For example, the first attempts to identify genes involved in melanoma metastasis employed cytogenetic technologies, comparing the karyotypes of tumour cell lines or tumour samples that exhibited metastatic or non-metastatic behaviour. More recently, several other genomic approaches and functional genomic analyses have been applied to achieve these goals[45].

Birkeland et al[46] have been able to analyse metastatic melanoma deposits from human patients by whole-exome-sequencing (WES) and revealed that most mutations are truncal events, with driver mutations (e.g. BRAF) almost completely shared between lesions, and other mutations (e.g. whole-genome duplication) arising as a late truncal event. By WES and whole-genome sequencing it has also been revealed by Furney et al that human mucosal melanomas are driven by different mechanisms from their cutaneous counterpart, in particular with a lack of UV-associated mutations and more copy number and structural variation in mucosal tumours[47]. Interestingly, BRAF V600E mutations are the most frequently identified in human cutaneous melanomas but only rarely (<6%) detected in their mucosal counterpart. This points out the need to study cutaneous and mucosal melanomas as two different entities, with different somatic mutation profiles. Therefore, there is the need to validate therapies specifically for each group of melanoma patients (cutaneous versus mucosal) to determine the efficacy of specific inhibitors (e.g. BRAF inhibitor).

The canine OMM genome has been recently the focus of some studies, with gene expression profiling proving to be a powerful tool for the identification of genes involved in metastasis[32]. In this study, primary oral malignant melanomas (OMMs) that metastasised were characterised by reduced expression of CXCL12 and increased expression of APOBEC3A compared to non-metastasising primary OMMs, potentially linking these genes to the metastatic process. However, genomic analysis of the metastatic process in canine OMMs is still in its infancy.

Aims:

- Investigate the molecular basis of canine OMM lymph node metastasis.
  Specific objective:
  Evaluate differences in gene expression between primary OMMs and relative regional lymph nodal metastasis by microarray mRNA profiling of 4 pairs of primary OMMs and lymph node metastases.

- Test the hypotheses that:
  (a) Immunohistochemical detection of lymphatic endothelial cells is more sensitive than haematoxylin and eosin staining at detecting vascular invasion of melanoma cells in canine primary OMMs with confirmed lymph node metastasis.
  (b) The presence of endothelial cell immunohistochemistry-detected lymphatic invasion is associated with canine OMM regional lymph node metastasis.
  (c) There is strong interobserver agreement in the detection of lymphatic invasion in canine primary OMMs.

Chapter 1

Gene expression profiling of canine primary OMMs and their lymph node metastases

Materials and methods:

Ethics Statements:

This study (Project number 59-2016) was approved by the Animal Health Trust (AHT) Ethics Committee. Informed, written consent was obtained from the owners of dogs whose oral melanoma and lymph nodal biopsies were included in this study. A melanoma/lymph node biopsy could be withdrawn from the study at any time. Patient treatment was unaffected by the study.

Tumour Samples:

Formalin fixed, paraffin embedded (FFPE) biopsies of canine primary OMMs and regional lymph node metastases from 4 dogs were retrieved from diagnostic histopathology archives [Pathology Department at the AHT (UK) and Department of Pathobiology at the University of Utrecht (Netherlands)]. These tissue biopsies were surgically excised from dogs (between 2012 and 2018) for treatment and staging purposes, respectively. The confirmed diagnosis of both primary OMMs and metastatic OMMs was obtained by microscopic examination of H&E stained sections by a board-certified pathologist (Di Palma S.), using a light microscope (Nikon Eclipse Ci). Histological evidence of lymph node metastasis was defined as the presence of large groups of neoplastic cells showing a mass effect on the lymphoid tissue, or the presence of small cohesive groups (more than 5 cells per high power field/400x) of pleomorphic cells containing melanin pigment. One single representative block was selected from each of the primary OMMs and their lymph node metastasis. Each block was selected on the basis of an area containing neoplastic cells in the corresponding H&E stained section examined. Each area was outlined using a fine-point permanent marker using a fine-point permanent (figure 1, left). A piece of Parafilm large enough to cover the region of interest was placed on the H&E stained slide. Using a fine-point permanent marker, we outlined the entire tissue and the region of interest within the tissue on the Parafilm. We transferred the marked Parafilm to the corresponding FFPE tissue block, matching the outline with the shape of the OMM tissue in the block. Using the tip of a permanent marker, we made shallow but visible indentations along the outline of the region of interest (figure 1, right).

Three tissue cores were extracted from the highlighted area of each FFPE block using a 3.0 mm Miltex Biopsy punch with plunger (Agar Scientific, UK).

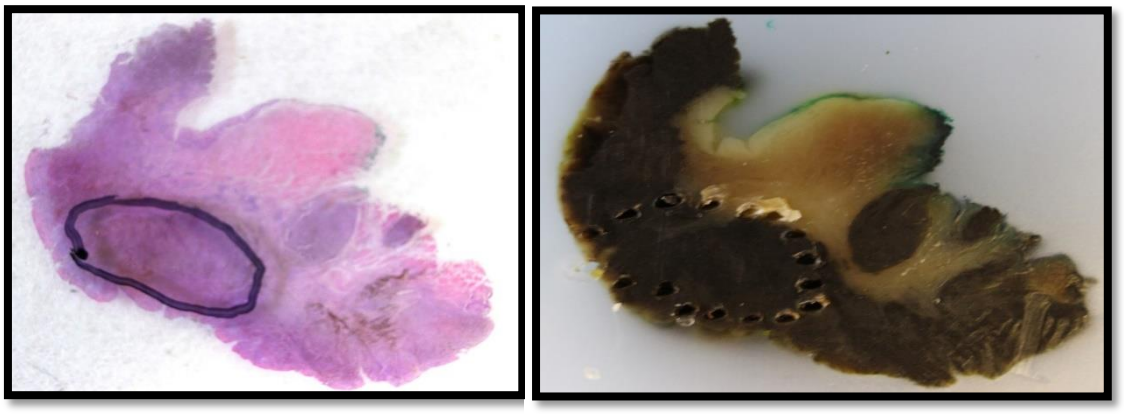

Figure 1: Left. H&E stained section of a primary canine OMM. The marked area identifies an area of interest containing melanoma neoplastic cells seen on microscopic examination. Right. Matched FFPE tissue block of tissue section shown in A, with area of interest outlined by multiple indentations.

RNA isolation, purification and quantification:

Total RNA was isolated from all three tissue cores obtained for each of the four FFPE primary OMMs and the four matched lymph node metastases using the RecoverAll Total Nucleic Acid Isolation Kit (Appendix 1). This kit has been used as it has been optimized for extraction of total nucleic acid from FFPE tissues and it is able to recover nucleic acids suitable for next generation sequencing, real-time RT-PCR, PCR, mutation screening and microarray analysis. OMM RNA samples were further purified (to remove melanin) by spin column filtration (OneStep PCR Inhibitor Removal Kit; Zymo Research, Freiburg, Germany) (Appendix 2). Total RNA concentration was measured for the selected primary and metastatic OMMs by spectrophotometry (NanoDrop 1000 Spectrophotometer, ThermoFisher Scientific, Paisley, UK) (Appendix 3), followed by fluorometry assay (Quant-iT RiboGreen RNA Assay Kit, ThermoFisher Scientific, Paisley, UK) (Appendix 4).

Quant-iT RiboGreen RNA Assay Kit uses advances fluorophores that become fluorescent upon binding to DNA or RNA. Therefore, this technology is more accurate compared to UV absorbance readings, as there is no interference from free nucleotides or other contaminants. NanoDrop assays have been used to confirm that RNA was isolated and these results helped to define how much an aliquot of each RNA sample should have been diluted for RiboGreen assays.

Global gene expression profiling:

RNA amplification, labelling and microarray hybridisation:

Fragmented, biotinylated single-stranded cDNA was prepared from 29 ng of each of the 4 FFPE primary OMMs and matched metastases RNA samples using the GeneChip WT Pico Reagent Kit (ThermoFisher Scientific, Paisley, UK) (Appendix 5).

A mixture of 4 unlabelled synthetic RNAs was added (at the beginning of the procedure) to each tumour RNA sample to act as 'labelling controls', and a mixture of 4 labelled bacterial DNAs was added (at the end of the procedure) to each labelled tumour cDNA sample to act as hybridisation controls

Each cDNA was individually hybridised to an array in a Canine Gene 1.1 ST Array Strip (ThermoFisher Scientific, Paisley, UK), in a proprietary hybridisation cocktail (ThermoFisher Scientific, Paisley, UK). Canine Gene 1.1 ST Array Strip has been used as it measures expression, across the entire gene, with higher resolution and accuracy than with classical 3`-biased microarray solutions, capturing transcript isoforms that may be missed with traditional methods. Array strip washing and streptavidin-phycoerythrin staining were undertaken by the GeneAtlas System (ThermoFisher Scientific, Paisley, UK) Fluidics Station, and array scanning by the GeneAtlas System (ThermoFisher Scientific, Paisley, UK)

Microarray data analysis:

Exon-level probe set expression values were generated by quantile normalisation, log2 transformation and signal summarisation, performed using the RMA algorithm (Summaries of Affymetrix GeneChip probe level data. Irizarry RA et al. Nucleic Acids Res. 2003 Feb 15;31(4):e15), implemented within 'Affymetrix Expression Console Software 1.3' (ThermoFisher Scientific, Paisley, UK). 'Outlier arrays' were considered to be those that had any single sample quality, labelling quality and hybridisation quality metric value ≥2 standard deviations away from the mean of the metric value for all the arrays (QC Metrics for Exon and Gene Design Expression Arrays. A summary based on the Affymetrix Quality Assessment of Exon and Gene Arrays White Paper, http://static1.1.
sqspcdn.com/static/f/1438485/21486054/1359060361517/qc_metrics_exon_gene_qrc.

pdf). Outlier arrays were excluded, and processing of the raw probe-level signal intensity data repeated to generate both quantile normalised and log2-transformed exon and gene-level probe set expression values. Gene-level probe sets ('Transcript clusters') with 'crosshyb_type' = 1 (unique hybridisation target) and 'category' = 'main' annotations (Affymetrix Exon and Gene Array Glossary, https://www.affymetrix.com/support/help/exon_glossary/index.affx), and for which at least 10% of its exons was 'present' (detection above background p-value <0.01; Affymetrix Exon Array Background Correction Revision Date: 2005-09-27, Revision Version: 1.0, https://assets.thermofisher.com/

TFS-Assets/LSG/brochures/exon_background_correction_whitepaper.pdf.) in at least ≥2 of the primary OMMs and ≥2 of the primary OMM lymph node metastases, were considered to be expressed and used for subsequent analyses.

Similarity between the global expression profiles of primary and lymph node OMMs was visualized by hierarchical clustering performed using Cluster[48]. Transcript clusters displaying statistically significant differential expression between primary and OMM lymph node metastases were identified by moderated T-test (p-value < 0.05) performed using the R Limma package[49,50]. P-values were adjusted by permutation testing[51] to compensate for "chance" p-values of 0.05 due to multiple testing. Differentially expressed transcription clusters were considered real when they showed a fold-change >2 (median OMM lymph node metastasis/median primary OMM expression value or median primary OMM/median OMM lymph node metastasis expression value).

Functional annotation enrichment analysis:

The biological processes and pathways overrepresented amongst genes displaying different expression between primary OMMs and OMM lymph node metastases were identified using DAVID[52,53]. The functional annotations associated with differentially expressed genes were compared with those ascribed to all Transcript clusters ('crosshyb_type' = 1 and 'category' = 'main') for which the expression of at least 10% of its exons was detected above background in ≥2% of the tumours in the primary OMMs and metastatic OMMs cohort, and over-represented biological processes and pathways identified.

Results:

Purity and quantity of total RNA isolated from FFPE OMM biopsies:

Nanodrop assay was used to determine the purity of RNA isolated from the canine OMMs. The purity of the RNA samples (as measured by the ratio of the absorbances at 260nm and 280nm, respectively, and the ratio of the absorbances at 260nm and 230nm, respectively) are illustrated in figures 2 and 3.

Both absorbance ratio assays for all samples confirmed the good quality of the isolated RNAs. Fluorometry assay with the Quant-iT RiboGreen RNA Assay Kit determined the concentration of RNA isolated from the canine primary and metastatic OMMs (figure 4).

The assay confirmed that the concentration of RNA in each of the OMM RNA samples was sufficient for use in the preparation of biotinylated single-stranded cDNA using the GeneChip WT Pico Reagent Kit (Appendix 4). The Kit recommends that 2 - 50ng of total RNA (in 3 µl, and therefore 0.67-16.67 ng RNA/µl) from FFPE tissue samples is employed. The RNA sample with the lowest concentration (sample 4P,9.56 ng RNA/µl) dictated that 28.68 ng of each RNA sample was employed to prepare biotinylated single-stranded cDNA for microarray hybridisation.

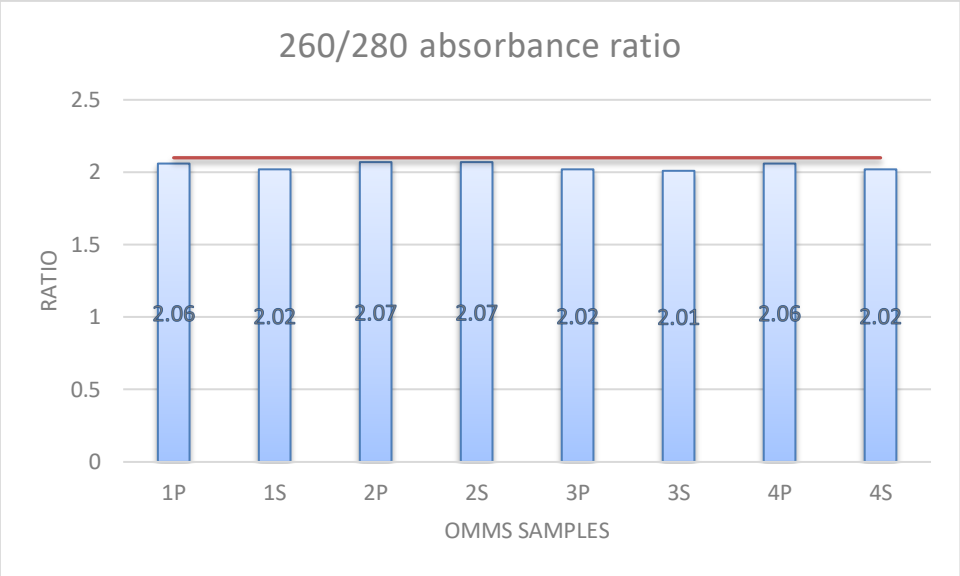

Figure 2: 260nm/280nm absorbance ratio for each of the primary (P) and metastatic (S) OMMs. The red line indicates the 'idealised' ratio for pure RNA. This value id indicative of an RNA sample with no protein contamination. (https://dnatech.genomecenter.ucdavis.edu/wp-content/uploads/2016/03/InterpretingSpectrometry.pdf)

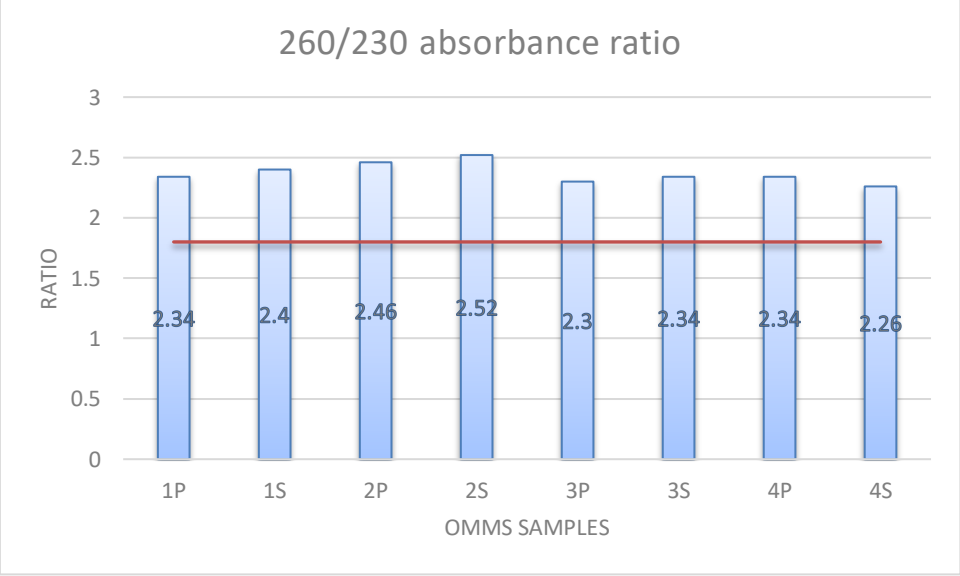

Figure 3: 260nm/230nm absorbance ratio for each of the primary (P) and metastatic (S) OMMs. The red line indicates the minimal acceptable value d (=1.8). An absorbance ratio below this value is considered to have a significant amount of contaminants (e.g. phenol, TRIzol, chaotropic salts) that can interfere with downstream applications. (https://dnatech.genomecenter.ucdavis.edu/wp-content/uploads/2016/03/InterpretingSpectrometry.pdf)

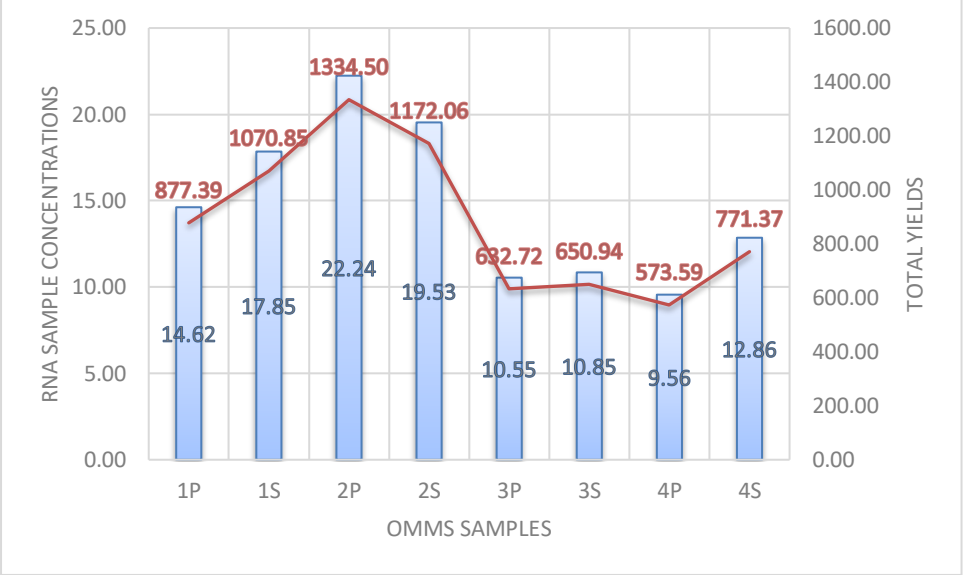

Figure 4: Undiluted concentration (expressed in ng/µl) and total yields (ng in 60 µl) of RNA for each of the primary (P) and metastatic (S) OMMs. The value of 60 µl is the volume of Nuclease-free water used to elute the RNA off a Filter Cartridge at the end of the RNA isolation procedure.

Tumours included in differential expression analysis:

In order to define gene expression patterns acquired by primary OMMs in the process of metastatic dissemination to the regional lymph node, we evaluated a cohort of canine primary (4) and metastatic (4) OMMs derived from surgically treated dogs. The use of matched primary and metastatic tumours was preferred in order to reduce sample genetic heterogeneity.

The microarray data for RNA sample 3S (metastatic tumour) was excluded from the analysis because it was an "outlier array" (see Materials and Methods), having an 'all_probeset_rle_mean' quality metric value 2.24 standard deviations away from the mean of the metric value of all the arrays.

The gene-level probe set expression values obtained for 4 primary and 3 metastatic OMMs were compared for 9,964 Transcript clusters (category = main; crosshyb_type = 1). A Transcript cluster was considered to be present if ≥10% of its exons were present both in ≥2 primary OMMs and ≥2 metastatic OMMs.

Genes displaying differential expression between primary and metastatic OMMs:

In total, 501 Transcript Clusters (genes) displayed a statistically difference in expression (p-value <0.05) between primary and metastatic OMMs, after permutation testing-adjustment. A >2-fold change (median primary/median metastatic expression value or median metastatic/median primary expression value) was considered to be authentic and more likely to be reproducibly measurable. A cohort of 158 Transcript Clusters fulfilling this requirement was identified for further analysis. In total, 141 genes (89%) showed higher expression in the metastatic OMMs compared to the primary OMMs, whereas only 17 genes (11%) were upregulated in the primary OMMs (figure 5).

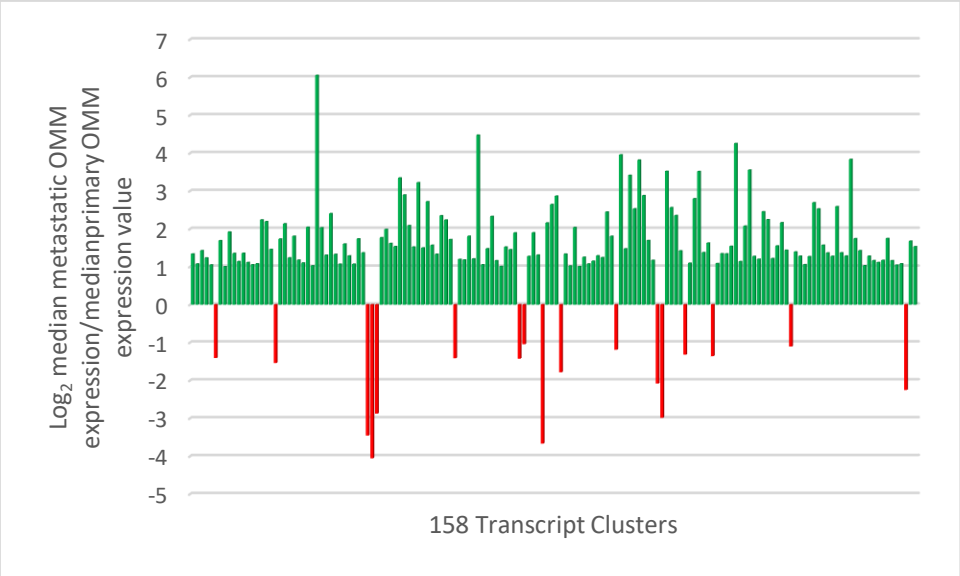

Figure 5: Genes differentially expressed between lymph node metastases and primary OMMs. Exon microarray-measured expression of 158 genes in 3 metastatic and 4 primary OMMs. The log_2-transformed metastatic/primary fold change (y-axis) denotes the difference in gene expression between the metastatic and primary OMMs.

Hierarchical clustering analysis assessed the similarity between the expression levels of the 158 differentially expressed Transcript Clusters across 4 primary and 3 metastatic OMMs (figure 6).

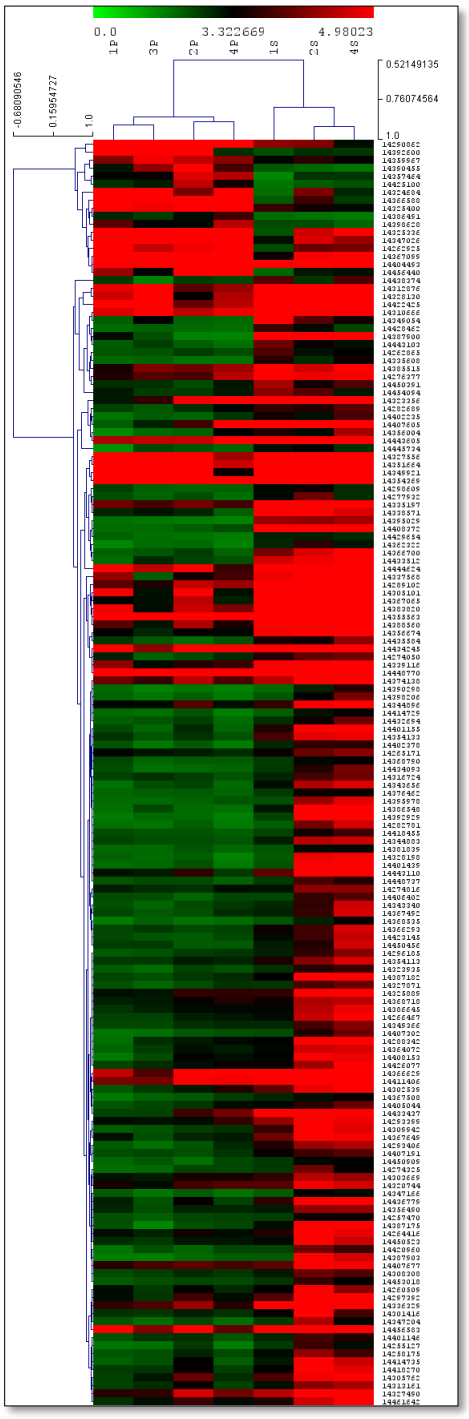

Figure 6: Hierarchical clustering analysis of 7 OMMs (4 primary and 3 metastatic) on the basis of 158 differentially expressed genes with significant p-value and fold-change. P: primary tumour. S: metastatic tumour.

Functional annotation enrichment analysis:

The frequencies of functional annotations assigned to 148 of the 158 Transcription Clusters that were differentially expressed between the primary and metastatic OMMs, and which had unique Ensembl canine gene IDs, were compared with those associated with all the Transcript Clusters expressed by the OMMs (9,123 of 9,964 which had associated Ensembl canine gene IDs). Over-represented amongst the genes exhibiting differential expression were 4 Gene Ontology Consortium biological processes and 4 KEGG pathways potentially involved in the metastatic process (table 1).

Functional annotation	Fold enrichment	P-value	Gene expression	
			M>P	P>M
GO:0045785~positive regulation of cell adhesion	15.187	0.015	*APBB1IP, VAV3*	*CYTH3*
GO:0030036~actin cytoskeleton organization	7.087	0.017	*ELMO1, CORO1A, DOCK2, FMNL1*	
GO:0001768~establishment of T cell polarity	47.249	0.041	*CCL19, DOCK2*	
GO:0007165~signal transduction	4.588	≤0.001	*TRAF5, ERBB2IP, SPOCK2, CDC42SE2, APBB1IP, LNPEP, FYB*	*SPARC*
Cell adhesion molecules (CAMs)	7.002	≤0.0001	*CD226, ICOS, PECAM1, DLA-DOB, ITGA4*	
cfa05200: Pathways in cancer	2.741	0.008	*TRAF5, IGF1, PLCB2, CDKN1B, JAK1, LEF1*	*ADCY2, MMP2*
cfa04062: Chemokine signaling pathway	4.951	≤0.001	*CCR7, PLCB2, ELMO1, CCL19, CXCL13, DOCK2, VAV3*	*ADCY2*
cfa04670: Leukocyte transendothelial migration	5.001	0.015	*PECAM1, VAV3, ITGA4*	*MMP2*

Table 1: Differentially expressed gene-associated enriched functional annotations. GO: Gene Ontology. M: Metastatic OMMs; P: Primary OMMs.

Discussion:

OMM is the most common malignant cancer of the oral cavity in the dog[5,6], with frequent metastases and low survival rate. The propensity of OMMs to metastasise is likely to be associated with changes in gene expression in tumour cells that negotiate the metastatic cascade[32]. However, little is known about genomic alterations that may be acquired by canine tumour cells during the "journey" to a lymph node, or a site of distant metastasis. Understanding of the basis of this process is fundamental as metastatic disease is the most common cause of cancer-associated death both in humans and in the canine species. Identification of these alterations could identify potential targets for control and treatment of OMM and its metastatic spread. For these reasons, we decided to evaluate the differences in gene expression between a cohort of canine primary OMMs and relative regional lymph nodal metastasis by microarray mRNA profiling.

As previously discussed, cell motility is fundamental for the metastatic process. Acquisition of a migratory phenotype by genomic alteration is putatively accounts for the ability of OMM cells to travel along lymphatic vessels and reach the regional/draining lymph node. Functional annotation enrichment analysis of genes differentially expressed between primary and metastatic OMMs has highlighted the key role of the control of cell motility by showing differential expression of genes involved in actin cytoskeleton organization, establishment of T cell polarity and leukocyte transendothelial migration.

Cell motility:

Several of the genes differentially expressed between primary and metastatic OMMs that are associated with cell motility are reported to be directly and/or indirectly involved in the regulation of the Rac1 pathway. These genes are also frequently correlated with highly aggressive tumours subtypes. In our study most of the genes show an increased expression in the metastatic site compared to the primary tumour, with subsequent potential higher activation of Rac1. As previously mentioned in the introduction, Rac1 represents one of the key players in cytoskeletal organization and cell migration.

Genes upregulated in canine OMM lymph nodal metastases that are involved in Rac1 regulation:

- *VAV3* is a member of the VAV gene family. The encoded VAV proteins activate pathways leading to actin cytoskeletal rearrangements, mainly acting as a guanine nucleotide exchange factor for RhoG, RhoA and Rac1 (uniprot.org/uniprot/Q9UKW4). Elevated VAV3 expression has been linked to prostate cancer progression and post-treatment recurrence[54].
- Dock2 is a member of the CDM family proteins, known to regulate actin cytoskeleton by functioning upstream of Rac[55]. DOCK2 activates RAC and regulates actin cytoskeleton through the interaction with ELMO1[56]. Proteins encoded by *ELMO1* interact with dedicator of cytokinesis proteins to promote phagocytosis and cell migration[57]. Mutation-effected aberrant activation of *ELMO1* and *DOCK2* has been reported in human oesophageal adenocarcinoma, a highly-invasive tumour prone to early metastasis[58].
- Coronin1A (encoded by *Coro1A* gene) seems to be a crucial component of the cytoskeleton in highly motile cells, functioning in forming protrusions of the plasma membrane involved in cell locomotion (uniprot.org/uniport/P31146). Overexpression of Coronin1A induces the translocation to the plasma membrane of Rac1 and favours its activation[59].
- Integrin alpha 4 (ITGA4) mediates cell-cell adhesion important in immune function (uniprot.org/uniprot/P13612). ITGA4 is also widely expressed in neural crest cells, leukocytes, striated and smooth muscle, and neurons, and mediates their migration, most likely co-localizing and activating Rac[60]. Moreover, ITGA4 expression has been demonstrated in human gastrointestinal stromal tumours (GISTs) and high expression has been associated with unfavourable prognosis[61].
- Chemokine ligand 19 (CCL19) binds to the chemokine receptor 7 (CCR7) and is involved in immunoregulatory and inflammatory processes (uniprot.org/uniprot/Q99731). Chemokines are also involved in all stages of tumour development due to their ability to induce cytoskeleton rearrangement, firm adhesion to endothelial cells and directional migration. For example, CCR7 expression in non-metastatic melanoma cell line renders it able to migrate to the lymph nodes in vivo[62] and the level of activated Rac was found to be

significantly increased after CCL19 treatment of human metastatic squamous cell carcinoma cell lines[63].

- We also found the end results of Rac1 pathway activation by detecting higher PLCB2 expression. Indeed, phospholipase C-β_2 (PLCB2) has an important role in intracellular transduction of many extracellular signals (uniprot.org/uniprot/A3KGF7). Activation of this molecule has been shown to be stimulated by Rac1 and other Rho GTPases[64].
- FMNL1 also showed increased expression in the metastatic OMMs, despite its inhibitory activity for Rac1. FMNL1 is part of the formin family proteins which are key regulators of actin and microtubule cytoskeletal dynamics (uniprot.org/uniprot/O95466). FMNL1 mediates the formation of F-actin networks and can organize actin filaments into bundles, interacting with Rac1 and RhoA. *FMNL1* silencing has been shown to increase Rac1 activity[65].
- *CDKN1B* also known as *p27Kip1* is a tumour suppressor that negatively regulates cell cycle progression (uniprot.org/uniprot/P46527). Selective deletion/inactivation of the *p27Kip1* gene is rarely found in human malignancies. Instead, p27 is often translocated from the nucleus to the cytoplasm and this translocation has been demonstrated to dramatically increase both cell motility and metastasis in vivo in a low metastatic melanoma cell line[66]. Moreover, p27 can directly promote cell invasion by facilitating invadopodia turnover via the Rac1/PAK1/Cortactin pathway[67].
- CDC42 Small Effector 2 (CDC42SE2, or SPEC2) is part of the family of Cdc42 effector proteins (uniprot.org/uniprot/Q9NRR3). Together with SPEC1, SPEC2 is strongly involved in coordinating and/or mediating Cdc42 signalling activities and weakly involved with Rac1[68]. In particular, they inhibit Cdc42-induced c-Jun N-terminal kinase (JNK) activation and induce formation of cell surface membrane blebs, not dependent on Cdc42 activity[68].

Genes downregulated in canine OMM lymph nodal metastases that are involved in Rac1 regulation:

- Downregulation of SPARC expression is related to the Rac1 pathway. Secreted protein acidic and cysteine rich (SPARC) is a matrix-associated protein, usually playing a role in bone mineralization, cell-matrix interaction and collagen binding (uniprot.org/uniprot/P07214). Its expression has been associated with aggressive, mesenchymal-like phenotype in a variety of human cancers, including melanoma. In particular its expression in melanoma cells was associated with decreased E-cadherin and increased N-cadherin expression levels suggesting that this protein may regulate epithelial–mesenchymal transition[69]. There is evidence that SPARC is a permissive factor for Rac1 that becomes fully active only when SPARC levels are low; indeed, suppression of SPARC expression induces the formation of lamellipodia extension[70].
- Matrix metallopeptidase 2 (MMP2) is able to cleave components of the extracellular matrix specifically gelatin type I and collagen types IV, V, VII and X (uniprot.org/uniprot/P08253). It has been shown that Membrane Type 1 Metalloprotease (MT1-MMP), highly expressed in neural crest cells, mediates human melanoma cell invasion through the activation of its target MMP2 and MMP2 activation is required to sustain RAC1 activity and promote cell migration[71].

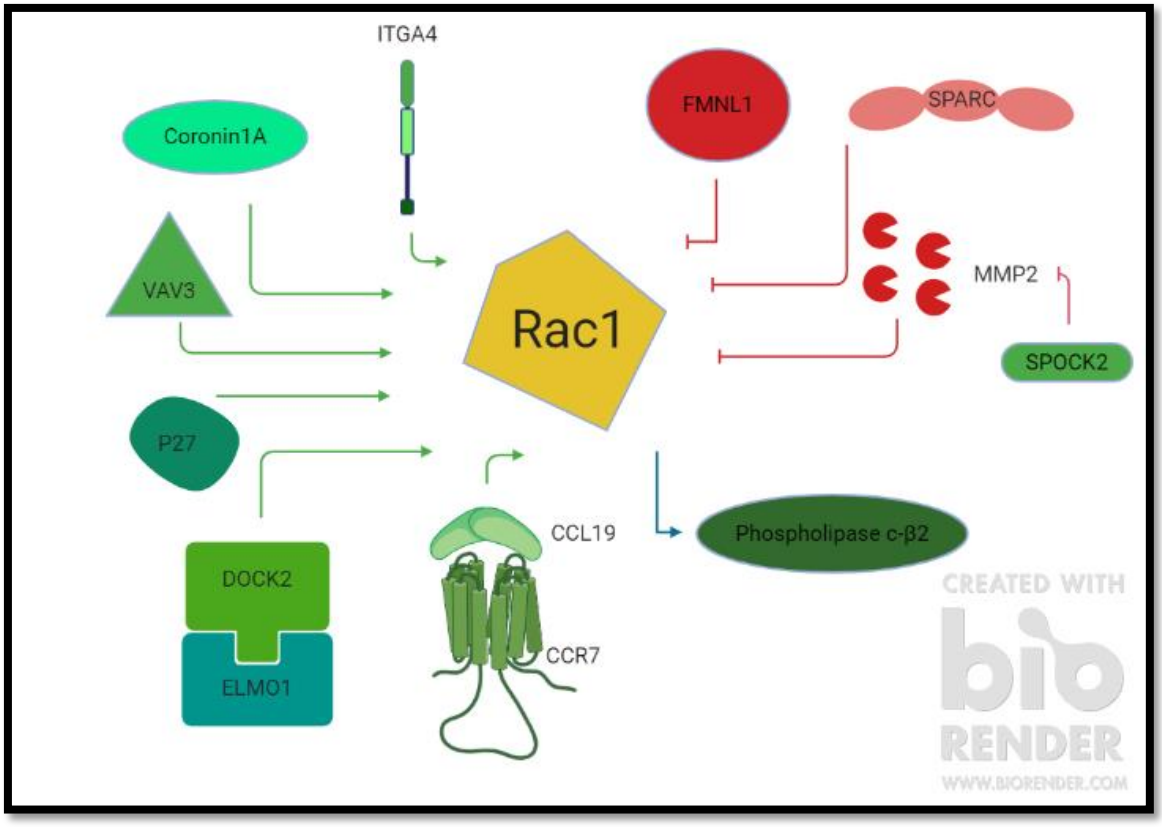

Figure 7: Rac1 pathway activating and inhibitory factors highlighted by differential gene expression and functional annotation enrichment analysis. Genes expressed at a higher level in metastatic OMMs compared to primary OMMs are highlighted in green and genes expressed at a lower level in metastatic OMMs in red. The arrow at the end of a line indicates activation of the target gene. A vertical bar at the end of a line indicates inhibition of the target gene.

Genes downregulated in canine OMM lymph nodal metastases that are apparently independent from the Rac1 pathway, but are involved in cell motility:

- Adenylate cyclase 2 (ADCY2) catalyses the formation of cAMP and mediates indirectly changes in gene expression patterns (uniprot.org/uniprot/Q08462). ADCY2 was shown to be enriched in the calcium signalling pathway and potentially being involved in the metastasis of human prostatic carcinoma[72]. Interestingly, calcium (Ca^{2+}) is a crucial regulator of cell migration, with a stable and transient gradient increasing from the front of migrating cells to the rear, promoting myosin II contraction[73]. However, Ca^{2+} influx has been linked to both increased and decreased migration, depending on cell types and stimuli[73]. Therefore, the significance of potential increased Ca^{2+} influx in our cohort of canine metastatic OMMs is unclear.
- SPOCK2, also known as testican-2, is a gene encoding a protein which binds with glycosaminoglycans to form part of the extracellular matrix. It is known that secreted SPOCK2 plays a significant role in the development and progression of several human cancers, mainly regulating the expression of Membrane Type 1 Metalloproteinase (MT1-MMP) and Matrix Metalloproteinase 2 (MMP2)[74]. Increased expression of SPOCK2 in the metastatic OMMs may explain the reduced expression of MMP2 in our study.

The Rac1 pathway and its role in melanoma metastasis:

Rac1 (Ras-related C3 botulinum toxin substrate 1) is the major ubiquitous isoform of Rac expressed in mammalian tissue, as part of the Rho family of small GTPases. This isoform controls assembly of the cellular actin cytoskeleton primarily via activation of the Scar/Wave complex (uniprot.org/uniprot/P63000). Lamellipodia (see Introduction) are actin polymerizations at the leading edge of cells, representing the main force for cell migration, and their formation is under the control of Rac1. Indeed, loss of Rac1 in tissues and cell cultures leads to the loss of lamellipodia and a general reduction of migration speed[42]. The results of the current study support the hypothesis that activation of the Rac1 pathway (downstream effectors and upstream regulators of Rac1) facilitates canine OMM cell migration to a regional lymph node.

Rac1 is implicated in epithelial-mesenchymal transition (EMT), inducing downregulation of E-cadherin and upregulation of N-cadherin, vimentin and snail1 in human cancers[75]. Melanocytes do not belong to the epithelial lineage and therefore the term EMT cannot be formally attributed to the progression of malignant melanoma. However, differentiated melanocytes do express E-cadherin and loss of this protein, which represents a hallmark of EMT in epithelial tumours is also evident in late stage malignant melanomas, especially in nodal metastases[76].

Rac1 is also involved in the transcriptional modulation of gene expression through NFkB, JNK and MAPK activation and later induction of AP-1 transcription factors involved in cell proliferation[77]. Novel activities of Rac1 have been recently described, such as regulation of the induction of DNA damage response mechanisms in cardiomyocytes[78] and involvement in vascular integrity and angiogenesis during blood vessel sprouting[79].

Rac1 has been identified as a novel candidate gene harbouring putative somatic mutations in human cutaneous melanomas. In particular the P29S hot spot mutation likely destabilises Rac1 favouring its active GTP-bound state[80]. Intriguingly, both $Rac1^{p29s}$ mutant melanomas cells and Rac1 wild type melanoma cells reduce their proliferation by downregulation of Rac1. These results suggest that Rac1 is a good target for therapy in human medicine, because it is active also in RAC1 wild type melanomas by other molecular events. Some of these events might be similar to the putative Rac1 pathway activation-promoting gene expression changes identified in the current study.

Despite the fact that the majority of the Rac1 pathway-associated differentially expressed genes were putatively positively regulating the Rac1 pathway, two genes, FMNL1 and MMP2, seemed to go against this trend.

To try to explain this apparent contradiction with activation of the Rac1 pathway and therefore of cell motility, we may think about the process of invasion and cell migration as a dynamic event, balancing between interaction/degradation of the extracellular matrix (by invadopodia) and cell movement (by lamellipodia). Indeed, although Rac1 is required for migration, high levels of Rac1 activity can impair migration[65]. Based on this hypothesis, we can speculate that the lymph node environment is most likely to be more favourable for a cell with an "exploration and invasion" phenotype rather than with an "adhesion and invasion" phenotype. The ability to degrade the extracellular matrix and interact with it is probably more important in the primary site, whilst the control of cell plasticity/motility seems to play a key role while reaching the lymph node. This hypothesis of a favourable "exploration and invasion" phenotype in metastatic dissemination is also supported by the higher expression of CDC42SE2 observed in the metastatic OMMs. Cdc42 small effector protein 2/SPEC2 inhibits Cdc42-induced cell shape changes[68]. As previously mentioned, Cdc42 is more involved in invadopodia rather than lamellipodia formation and lamellipodia are a key feature of the "exploration and invasion" phenotype.

Cell interactions:

A fundamental property of neoplastic cells is the ability to interact with other cells, driving/controlling them in order to favour tumour survival and dissemination. Several of the genes shown to be upregulated in metastatic OMMs in this study encode surface molecules that interact with endothelial cells and inflammatory cells. Elevated expression of these genes is potentially associated with a specific phenotype that confers a selective advantage. Indeed, neoplastic cells able to interact with both lymphatic vessels and the lymph node environment are most likely to be able to survive during their migration.

Genes upregulated in canine OMM lymph nodal metastases that are involved in cell-cell interactions:

- FYB, also known as the adhesion and degranulation promoting adapter protein, positively mediates T cell receptor-dependent as well as integrin-mediated cell adhesion (uniprot.org/uniprot/O15117). Overexpression of FYB has been correlated with ductal carcinoma in situ progression to intraductal carcinoma and breast cancer metastasis in humans[81].
- *CD226* encodes a glycoprotein expressed on the surface of NK cells, platelets, monocytes and a subset of T cells. This protein mediates cellular adhesion of platelets and megakaryocytic cells to vascular endothelial cells (RefSeq, Jan 2015). A similar interaction with endothelial cells can be hypothesised for neoplastic cells expressing this molecule.
- Platelet/endothelial cell adhesion molecule 1 (PECAM1) is expressed on the surface of several cell types including platelets, leukocytes and endothelial cells. In one study, a subpopulation of PECAM1+ melanoma cells have been identified. These cells were more motile than PECAM1- melanoma cells and were able to form vascular-like structures (vasculogenic mimicry)[82].
- APBB1IP (Amyloid Beta Precursor Protein Binding Family B Member 1 Interacting Protein) is also known as the RIAM (Rap1-GTP-interacting adaptor molecule), and appears to be involved in actin cytoskeletal remodelling (uniprot.org/uniprot/Q7Z5R6). The RIAM/integrin/talin complex has been shown to localise at the tips of growing actin filaments in lamellipodial and filopodial protrusions, acting like “sticky fingers” at the leading edge of migrating cells[83].
- Chemokine C-X-C motif ligand 13 (CXCL13) is a chemotactic protein for B cells, interacting with the receptor CXCR5 (uniprot.org/uniprot/Q99616). In a study focusing on CXCL13 expression in melanocytic cells, CXCL13 was strongly expressed in a minor subpopulation of tumour cells in primary melanoma, while a greater fraction of cells in the metastatic melanoma tissue expressed this protein. In the same study, CXCL13 was not detected in normal human epidermal melanocytes *in situ* therefore suggesting a potential role as both a specific biomarker for melanoma and a therapeutic target[84].

- DLA-DOB is a MHC class II molecule, usually expressed on antigen-presenting cells (uniprot.org/uniprot/Q5W418). However, recent studies have shown that these molecules are expressed in almost 50% of human melanoma and they can increase migration and invasion of melanoma cells[85].
- Lymphoid enhancer-binding factor-1 (LEF1) is usually expressed in lymphoid cells. However, in one study, expression of the encoded protein has also been demonstrated in human melanoma cell lines and correlated to different phenotypes. Interestingly, expression of LEF1 is high in proliferative phenotype human melanoma cells *in vitro* and relatively low in low proliferative/high invasive populations. Apparently, the human metastatic phenotype lightly reduces the expression of LEF1[86]. These results contrast with that of the present study, where LEF1 was found to exhibit a 3-fold higher level of expression in the lymph node metastases than in the primary OMMs.

Cancer progression and cell survival:

As previously mentioned (see Introduction), eight alterations of normal cell physiology are essential to determine a malignant phenotype[30]. In regard to tissue invasion and metastasis, the results of the present study suggest that changes in gene expression in metastasising OMM cells promote increased cell motility assisting travel within the lymphatic system. Metastasising OMM cells also express certain proteins that enhance their interactions with other cells and the surrounding environment. In addition, a number of the genes shown to be differentially expressed between the primary tumours and lymph node metastases may be involved in metastatic spread via increasing cell survival and regulating angiogenesis.

Upregulated genes in canine OMM lymph nodal metastasis involved in cancer progression and cell survival:

- Several studies have focused on TRAF5 (tumour necrosis factor receptor-associated factor 5) due to its pivotal role in cancer progression. For example, upregulation of TRAF5 has been confirmed in human gastric cancer tissue[87], down-regulated TRAF5 caused significant inhibition of cell proliferation and promotion of apoptosis in melanoma cell[88] and its tumour-promoting activity has been demonstrated for colorectal cancer[89].
- ERBB2 interacting protein (ERBB2IP) binds to the receptor tyrosine-protein kinase ERBB-2, mainly in epithelia, regulating its function and localisation and leading to uncontrolled cellular proliferation and oncogenesis (uniprot.org/uniprot/Q80TH2). ERBB2IP has been reported to contribute to the tumorigenesis of human hepatocellular carcinoma[90]. Moreover, ERBB2 amplifications and mutations have been reported in human melanomas (including the mucosal subtype) and clinical trials assessing response to targeted therapy for ERBB2-altered melanomas are currently ongoing[91].
- Insulin-like growth factor 1 (IGF-1) is a hormone similar to insulin but with a much higher growth-promoting activity (uniprot.org/uniprot/P05017). IGF-1 has been identified as a key driver of cell proliferation, in the development and growth of multiple tumours and in the prevention of apoptosis. In particular, IGF-1 inhibition has been shown to reduce the stemness features and functional characteristics of melanoma-initiating cells[92].
- *JAK1* encodes a tyrosine kinase involved in the IFN-alpha/beta/gamma signal pathway (uniprot.org/uniprot/P23458). JAK1 is able to activate STAT5, a signal transducer and activator of transcription that is frequently activated in human patients with cutaneous melanoma metastases[93]. STAT5 plays a key role in malignant transformation of haematological malignancies, breast, prostate and human non-small cell carcinoma[93].

Genes downregulated in canine OMM lymph nodal metastases that are involved in cancer progression and cell survival:

- CYTH3 (also called Grp1) is a guanine nucleotide exchange factor that facilitates the exchange of GDP for GTP to generate the active form of ADP Ribosylation Factor 6 (*ARF6*). Arf6 has been shown to be essential for the activation of Hepatocyte Growth Factor-induced tumour angiogenesis[94] (. In this study, increased expression of CYTH3 at the primary site is consistent with the need for a blood supply to support primary tumour growth.

Leucyl-cystinyl aminopeptidase (*LNPEP*, or *hPLAP*) is associated with the 'signal transduction' Gene Ontology Consortium Biological Process annotation that is over-represented amongst the functional annotations assigned to the genes differentially expressed between the primary OMMs and lymph node metastases (Table 1). *LNPEP* encodes a protein that cleaves vasopressin, oxytocin and other peptide hormones (uniprot.org/uniprot/Q9UIQ6). It displays elevated expression in the lymph node metastases in this study, but its role in the development of human melanoma is unclear[95], and further studies are needed to elucidate its potential role in tumour progression and metastatic dissemination.

Conclusions:

This study has demonstrated that canine OMM lymph node metastases are characterised by increased expression (relative to primary OMMs) of a set of genes involved in cell motility, cell interactions with the surrounding environment, and cell survival. On the basis of these results, all these gained/improved capabilities seem to be fundamental for the migration, and survival during migration, of neoplastic melanoma cells during dissemination through the lymphatic system and production of lymph nodal metastases. The potential key role of Rac1 and its upstream activators and downstream effectors in the modulation of critical elements of metastasis has been highlighted, as has previously been done in human medicine[96]. It is possible that melanoma cells are able to disseminate to distant sites due to re-acquisition of plastic and highly migratory behaviour characteristic of their embryonic precursors[34]. However, neoplastic melanocytes are possibly also able to apply mechanisms used by other cell

lineages to succeed in the metastatic journey. Rac1 pathway activation could be one of these mechanisms as it is essential for lamellipodia formation. Indeed, lamellipodia formation is used by dendritic cells to interact with the endothelium, polarise and actively crawl toward the draining lymph node[97].

The role of Rac1 and its pathway in tumorigenesis, angiogenesis, invasion, and metastasis has been proven for several different human tumour types[96], and it may have a similarly important role in canine OMM development and progression. Targeting Rac1 and its regulatory network would be beneficial for cancer treatment, but this has unfortunately proved to be difficult. Rac1 signalling is involved in many processes of normal cell physiology, like cellular plasticity, migration and invasion, cellular adhesions, cell proliferation, apoptosis, reactive oxygen species (ROS) production and inflammatory responses[98]. Therefore, targeting Rac1 in a clinical setting might have undesirable side effects. Investigation of both the downstream effectors and the upstream regulators of Rac1 could indicate the best unimodal/multimodal therapeutic approaches for canine OMMs. At this stage additional validation in different preclinical cancer models is needed to supplement the striking *in vitro* evidence of the benefits of targeting Rac1[99].

Limitations of the study:

The main limitation of this study is the relatively low number of OMM primary and lymph node metastasis biopsy pairs analysed. Fine needle aspiration (FNA) remains a mainstay diagnostic technique when evaluating for metastasis to regional lymph nodes in animals, including cancer staging in dogs with OMMs. FNA is less invasive compared to surgical excision and is frequently preferred to histological examination of the lymph node for this reason, despite the latter technique being considered to be the gold standard for identifying lymph node metastasis[100]. Therefore, only a few cases were found where both the primary canine OMM FFPE tissue and a matched lymph node metastasis was available.

Furthermore, FFPE biopsies of primary and metastatic canine OMMs were used in the study. Degradation of RNA by formalin fixation is well known, and probably mainly affects accurate quantification of genes expressed at low levels. However, reliable data has been obtained by Affymetrix microarray-based gene expression profiling of FFPE tissues[101].

Future work:

The differential expression of 12 genes involved in the Rac1 pathway identified by microarray mRNA profiling will be validated by quantitative Reverse transcription-Polymerase Chain Reaction assay. Gene expression will be assayed in the 4 pairs of primary and lymph node biopsies utilised in the microarray study, and in a further 9 pairs of primary canine OMMs and their lymph node metastasis.

The comparative global gene expression profiling of primary OMMs and their lymph node metastases will be extended by RNA-sequencing of the additional 9 pairs of tumour biopsies. The objective will be to identify genes that show a consistent difference in expression between the primary and the metastatic tumours, and also genes which are recurrently affected by functionally-relevant exonic mutations that are unique to the metastatic tumours.

Chapter 2

Lymphatic invasion in canine oral melanoma: can the sensitivity of detection be increased by Prox-1 immunohistochemical staining for lymphatic endothelial cells?

Materials and methods:

Ethics Statements:

This study (Project number 33-2017) was approved by the Animal Health Trust (AHT) Ethics Committee. Informed, written consent was obtained from the owners of dogs whose primary oral melanomas were included in this study. A primary melanoma biopsy could be withdrawn from the study at any time. Patient treatment was unaffected by the study.

Tumour Samples:

Formalin fixed, paraffin embedded (FFPE) biopsies of canine primary OMMs from 21 dogs (10 with a metastatic and 11 with a non-metastatic tumours) were retrieved from diagnostic histopathology archives [Pathology Department at the AHT (UK) and Department of Pathobiology at the University of Utrecht (Netherlands)]. The tissue biopsies were surgically excised from dogs (between 2012 and 2018) for treatment purposes. Eighteen representative FFPE blocks containing different areas of the primary neoplastic masses were selected for both the metastasising and non-metastasising cases, totalling 36 tissue blocks. Metastatic and non-metastatic states were assessed by FNA and/or histopathology of the regional/draining lymph node and they were defined as the presence or absence of neoplastic melanoma cells in the lymph node, respectively.

Evaluation of lymphatic invasion:

Haematoxylin and eosin staining (H&E) and immunohistochemistry (IHC) for a lymphatic-specific marker, Prox-1 (AngioBio, Del Mar, CA, USA) (Appendix 6) were performed on each selected FFPE tissue block for evaluation of lymphatic invasion by melanoma cells. Confirmation of species cross-reactivity for Prox-1 antibody for FFPE canine tissue has been previously reported by Halsey et al[23]. We validated the antibody in our laboratory checking for presence of positive nuclear signal on efferent and afferent lymphatics in normal canine FFPE mesenteric lymph nodes and lacteals in normal canine small intestine. Negative controls, omitting the primary antibody, were included to assess non-specific background staining.

The intratumoural (IT) and peritumoural (PT) presence of lymphatic invasion was blindly assessed by three pathologists (Brunetti B, Avallone G, Pellegrino V), using different optical microscopes (Leica DMLB100T, Optika B-350, Optika B-382PL respectively), but all with the same ocular lens field number (FN20).

Evaluation of the stained sections (H&E and IHC) was performed following these criteria:

- Avoid areas of necrosis.
- Lymphatic vessels are defined as structures with a complete luminal profile lined by endothelial cells on H&E and structures lined by endothelial cells with complete nuclear positive staining on immunohistochemistry for Prox-1.
- Lymphatic invasion is defined as the attachment of melanoma cells (single or in clusters) to the luminal side of endothelial cells or free in the vascular lumen.
- Scoring is based on “lymphatic invasion” or “absence of lymphatic invasion”. Doubtful invasion has to be considered “absence of lymphatic invasion”.
- The evaluation of lymphatic invasion has to be performed on an entire section containing the tumour and peritumoural area, scanning at 100X magnification and checking for suspect areas of invasion at 400X magnification on optical microscope. No evaluation of non-neoplastic tissue outside the PT area is required.
- The PT area is defined as non-neoplastic tissue present within 10 microscopic fields (400x magnification) from the tumour borders.

Statistical analysis:

The Kuder Richardson Coefficient of reliability (K-R 20) test was used to assess the degree of concordance between the three pathologists in determining the absence or presence of lymphatic invasion. The K-R 20 test value was interpreted as follow:

K-R 20 value	Degree of agreement
<0.2	poor
0.21-0.4	fair
0.41-0.6	moderate
0.61-0.8	strong
>0.8	near complete agreement

Concordance analysis was performed on “single slides” (all slides obtained from the selected OMMs) and “cases” (when more than one slide was available for the same tumour, they were grouped together and considered as a single case).

Different analyses were performed based on:

- Evaluation of only H&E-stained sections
- Evaluation of only Prox-1 immunostained sections
- A combination of the H&E and Prox-1 IHC evaluations
- IT and PT area evaluations for each of the 3 previous groups

Results:

Interobserver agreement on lymphatic invasion in canine primary OMMs:

The degree of agreement between the three pathologists in determining the presence or absence of lymphatic invasion in primary OMM sections was calculated. Detection of lymphatic invasion in a cohort of 10 metastatic and 11 non-metastatic canine OMMs was performed on a total of 36 H&E stained sections (figure 8) and 36 Prox-1 IHC-stained sections (figure 9). Lymphatic vessels were detected in IT and PT areas both on H&E stained and Prox-1 IHC stained sections. Table 2 shows results of the readings.

Case ID	Lymph node metastasis	No. of primary tumour sections analysed	Lymphatic invasion											
			Intratumoral						Peritumoral					
			H&E			IHC Prox-1			H&E			IHC Prox-1		
			P1	P2	P3	P1	P2	P3	P1	P2	P3	P1	P2	P3
1	Yes	3	No	No	No	No	No	No	No	Yes	No	No	Yes	No
2	Yes	2	No	No	No	No	No	No	No	Yes	No	No	No	No
3	Yes	5	No	Yes	Yes	No	Yes	Yes	Yes	Yes	Yes	Yes	Yes	Yes
4	Yes	2	No	No	Yes	No	No	No	Yes	No	Yes	No	No	Yes
5	Yes	1	No	No	No	No	No	No	No	No	No	No	No	No
6	Yes	1	No	No	No	No	No	No	No	No	No	No	No	No
7	Yes	1	No	No	No	No	No	No	Yes	No	Yes	No	No	No
8	Yes	1	No	No	No	No	No	No	No	No	No	No	No	No
9	Yes	1	No	Yes	Yes	No	Yes	Yes	No	Yes	Yes	No	Yes	Yes
10	Yes	1	No	No	No	No	No	No	No	Yes	Yes	No	No	Yes
11	No	4	Yes	No	No	No	Yes	No	Yes	No	No	No	No	No
12	No	2	No	No	Yes	No	No	No	No	No	No	No	No	No
13	No	3	No	No	No	No	No	Yes	No	No	Yes	No	Yes	No
14	No	2	No	No	No	No	No	No	No	No	No	No	No	No
15	No	1	No	No	No	No	No	No	No	No	No	No	No	No
16	No	1	No	No	No	No	No	No	No	No	No	No	No	No
17	No	1	No	Yes	Yes	Yes	No	No	No	No	No	No	No	No
18	No	1	No	No	No	No	No	No	No	No	No	No	No	No
19	No	1	No	No	No	No	No	No	No	No	No	No	No	No
20	No	1	No	No	No	No	No	No	No	No	No	No	No	No
21	No	1	Yes	Yes	Yes	No	Yes	No	No	No	No	No	No	No

Table 2: Presence (Yes) or absence (No) of lymphatic invasion reported by all three pathologists for each "case". P1: pathologist 1; P2: pathologist 2; P3: pathologist 3.

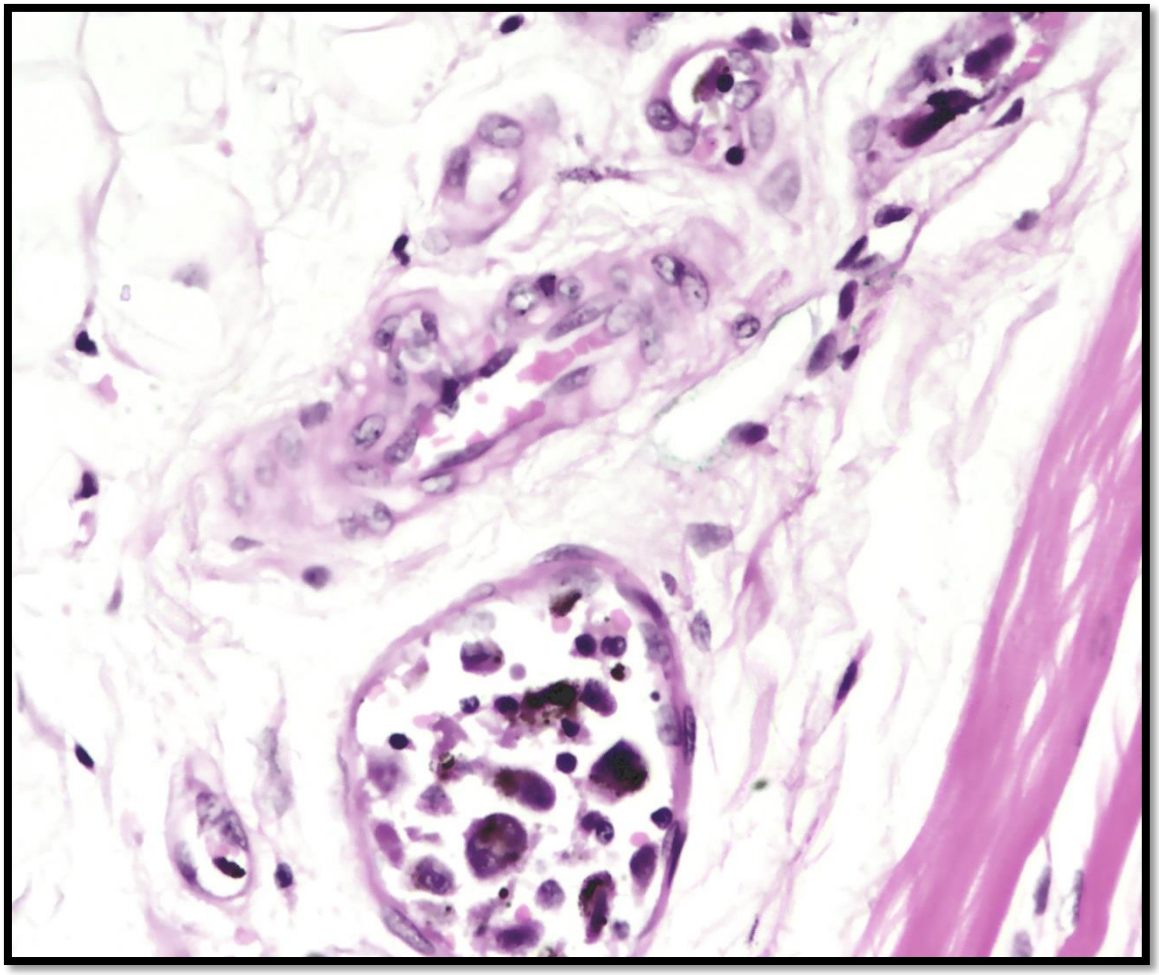

Figure 8: Melanoma cells in the lumen of a vascular structure (most likely a lymphatic vessel based on the features of the vascular wall and almost complete absence of erythrocytes in the lumen). H&E staining, 400x.

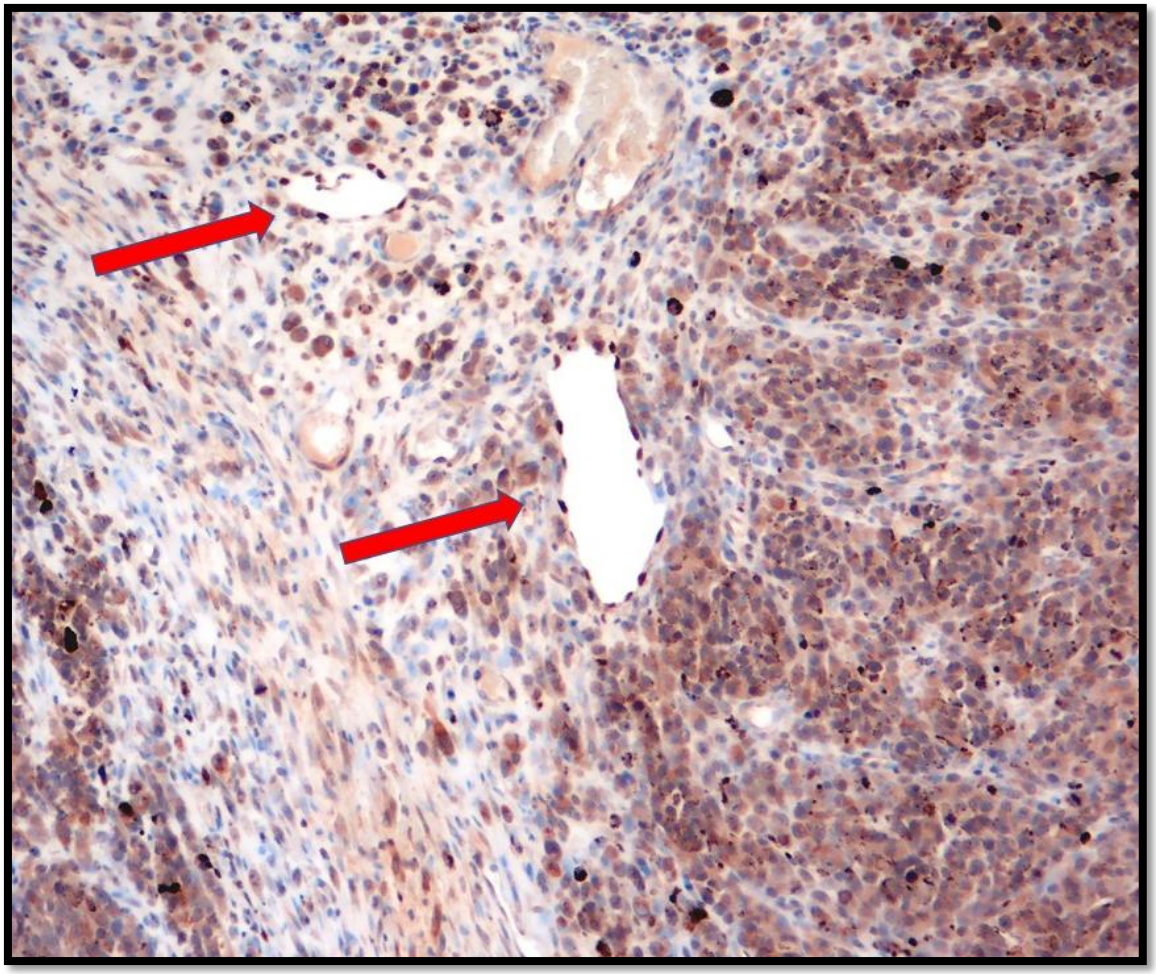

Figure 9: Strong positive nuclear signal for Prox-1 in endothelial cells in some vessels (red arrows), with no obvious presence of intraluminal melanoma cells. IHC for Prox-1, 100x

Based on H&E stained sections, the degree of agreement upon evaluation of “cases” was always higher (moderate to strong) than that achieved through evaluation of “single slides” (fair to moderate), independent of the area(s) selected (IT, PT, IT+PT). The highest degree of agreement (0.68/strong) was achieved in IT areas for “cases”. The lowest degree of agreement (0.35/fair) was achieved for “single slides” when focussing in PT areas. The values obtained from the K-R 20 test are detailed in figure 10.

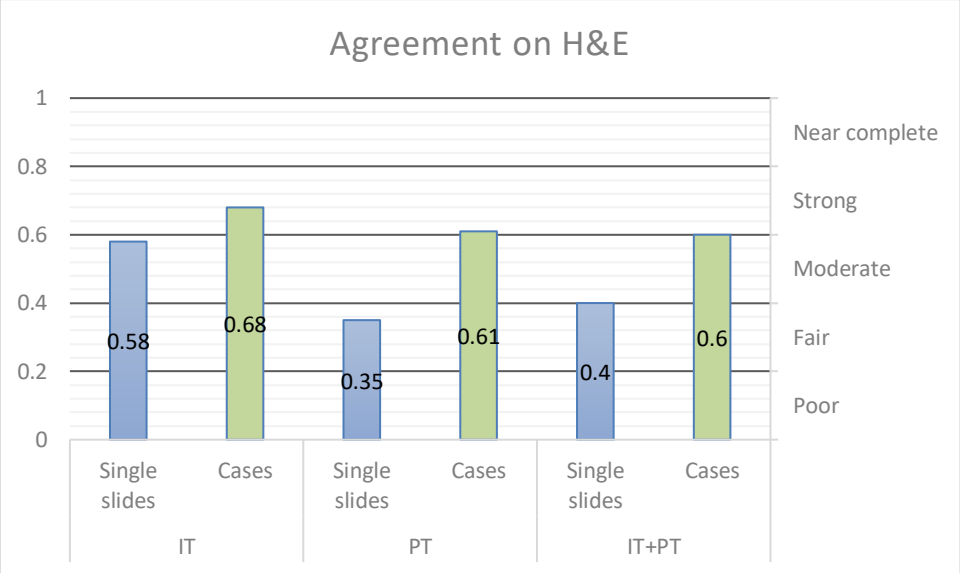

Figure 10: The degree of agreement in regard to the identification of lymphatic invasion in H&E-stained primary OMM sections measured by the K-R 20 test. IT: intratumoural; PT: peritumoural; IT+PT: intratumoural + peritumoural areas.

Similar results were obtained by examination of IHC sections stained with Prox-1. Indeed, higher degree of agreement was achieved on evaluation of IHC-stained "cases" (fair to strong) compared to "single slides" (poor to fair). The highest degree of agreement (0.72/strong) was achieved in PT areas for "cases". The lowest degree of agreement (0.17/poor) was achieved on "single slides" from IT areas. Detailed values are depicted in figure 11.

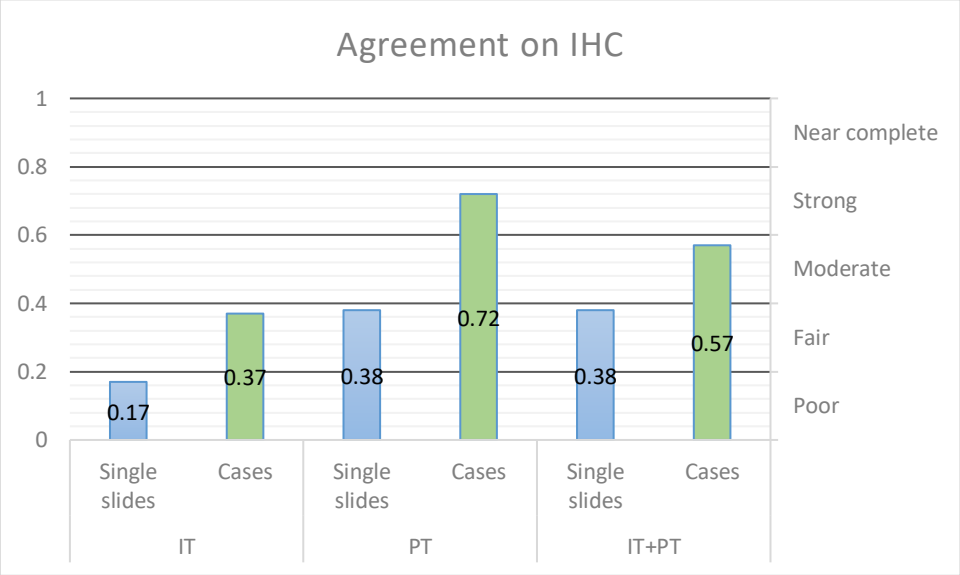

Figure 11: The degree of agreement in regard to the identification of lymphatic invasion in Prox-1 IHC-stained primary OMM sections measured by the K-R 20 test. IT: intratumoural; PT: peritumoural; IT+PT: intratumoural + peritumoural areas.

Finally, combining evaluation of lymphatic invasion from H&E and Prox-1 IHC-stained sections, the degree of agreement was strong for “cases”, and fair to moderate for “single slides”. The highest degree of agreement (0.76/strong) was achieved for “cases” in IT areas and the lowest (0.38/fair) for “single slides” in PT areas. the K-R 20 test values are depicted in figure 12.

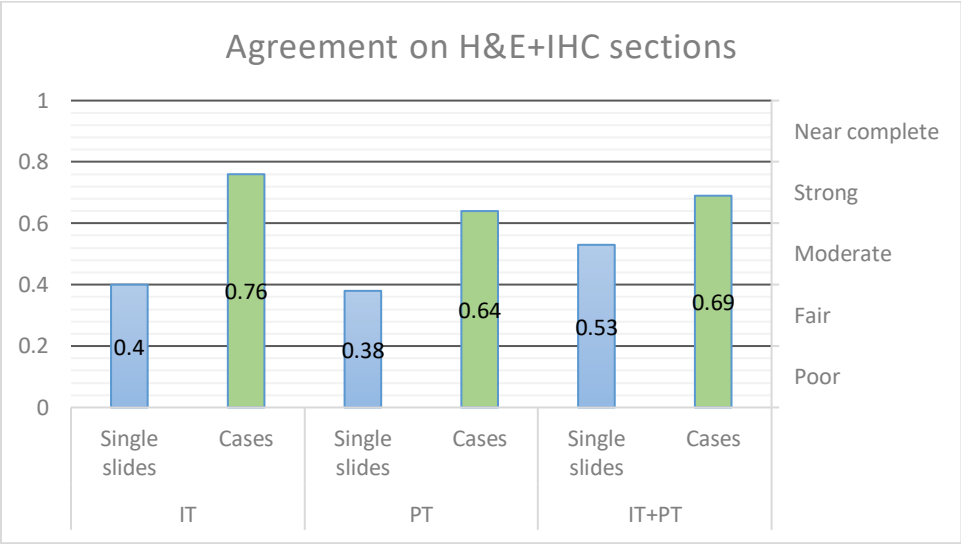

Figure 12: The degree of agreement in regard to the identification of lymphatic invasion in H&E and Prox-1 IHC-stained measured by K-R 20 test. IT: intratumoural; PT: peritumoural; IT+PT: intratumoural + peritumoural areas.

The highest degree of agreement between the three different pathologists was achieved with evaluation of H&E+IHC “cases”, even though there was no significant difference compared to the evaluation of only H&E “cases” (strong agreement in both evaluations for all areas, except for a moderate agreement on H&E in IT+PT areas). The trend of agreement based on “cases” matched the trend on “single slides”.

Sensitivity and specificity of detection of lymphatic invasion in predicting lymph nodal metastasis:

Sensitivity and specificity have been calculated on the category (lymphatic invasion present or absent) assigned most often by examination of H&E and Prox-1 IHC-stained sections of a given primary OMM by all three pathologists. As microscopic examination

of all sections available from an OMM better reflects the real daily diagnostic setting, we decided to include only “cases” and not “single slides” in this analysis. Table … shows detailed results.

In this study, lymphatic invasion was detected in 12 “cases” in total with examination of H&E stained sections. Unexpectedly, using Prox-1 IHC, only 8 “cases” with lymphatic invasion were detected. Combined use of H&E and IHC did not increase detection of lymphatic invasion (12 “cases”), being all “cases” stained with Prox-1 detected with H&E stained sections.

The sensitivity in predicting lymph nodal metastasis by evaluation of H&E or Prox-1 IHC-stained IT areas was low, ranging from 13.3% to 46.7%. Higher sensitivities were obtained from the evaluation of PT and IT+PT areas.

On the other hand, specificity was high, with consequent low numbers of false positives (67%-97% specificity). Higher results were achieved with examination of PT areas (91-97% specificity).

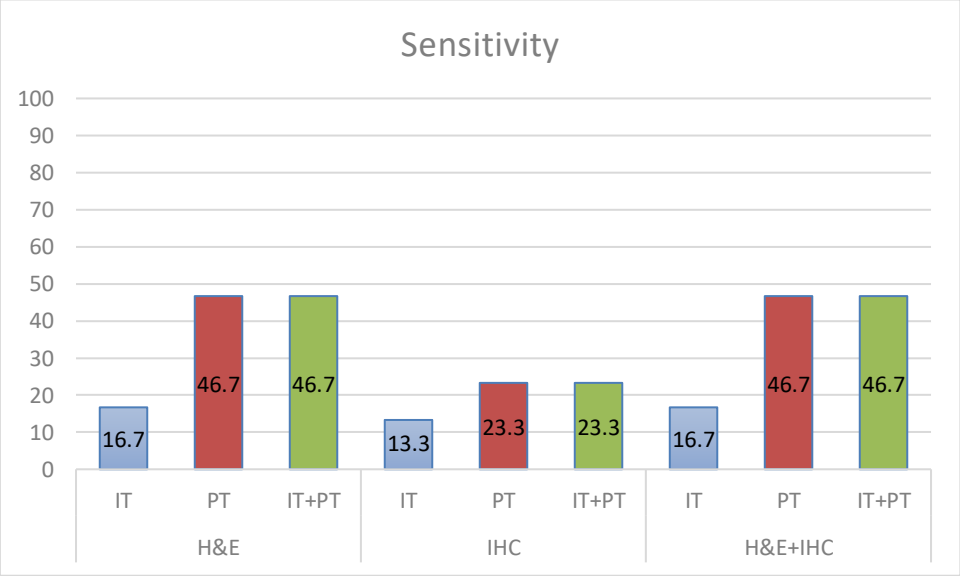

Figure 13: Sensitivity of predicting regional lymph node metastasis by lymphatic invasion assessed by H&E-staining, Prox-1 IHC, or the two combined. IT: intratumoural area; PT: peritumoural areas; IT+PT: intratumoural + peritumoural areas.

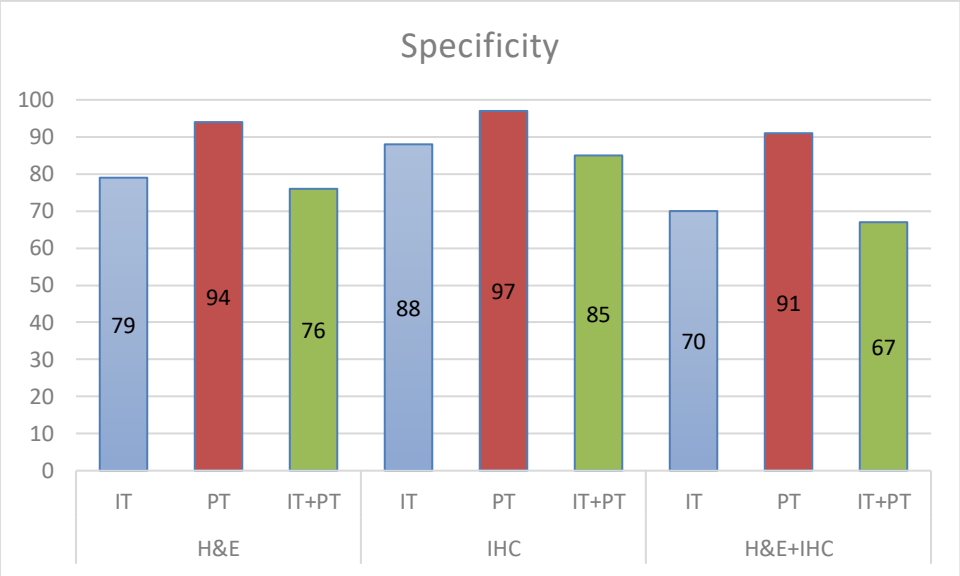

Figure 14: Specificity of predicting regional lymph node metastasis by lymphatic invasion assessed by H&E-staining, Prox-1 IHC, or the two combined. IT: intratumoural area; PT: peritumoural areas; IT+PT: intratumoural + peritumoural areas.

Discussion:

The presence of LVI in a primary tumour is generally considered an unfavourable prognostic factor for several human cancers[14–17]. In addition to LVI, either lymphatic vessel invasion or blood vessel invasion individually are reported to be prognostic[15].

The prognostic value of lymphatic invasion detected in H&E-stained sections from the primary site has also been demonstrated in dogs with oral and cutaneous melanocytic tumours[18].

The clinical relevance of enhanced detection of LVI by immunohistochemistry has been proven in human melanomas, with IHC-detected LVI more significantly associated with adverse clinicopathologic variables than LVI detected by routine histology[14]. IHC staining has also been shown to increase the sensitivity of lymphatic invasion detection by up to nine-fold compared to that achieved by H&E staining[20].

Therefore, this study set out to evaluate if the use of IHC for lymphatic vessels could also be applied in the veterinary field for increasing the detection of lymphatic invasion by neoplastic cells, specifically those derived from canine primary OMMs.

The use of Prox-1 as a marker for lymphatic invasion was chosen due to the reported cross-reactivity of an antibody raised against the human Prox-1 protein in canine FFPE tissue and the better performance of the antibody in regard to signal strength and background staining, compared to other markers (see Introduction).

Unexpectedly, in this study the use of Prox-1 IHC did not improve the detection of lymphatic invasion by neoplastic melanocytes in canine primary OMM sections beyond that achieved by H&E staining. Indeed, lymphatic invasion was detected in a larger number of primary OMMs by evaluation of H&E stained sections than by evaluation of Prox-1 IHC sections. These results contrast with those of several previous studies that have found that the use of IHC for specific lymphatic markers increased the detection of lymphatic invasion[19,102].

The lack of efficacy of Prox-1 IHC at detecting lymphatic invasion in primary OMMs in this study may be due to several factors. A positive IHC signal might have been “hidden” in the melanoma samples. Indeed, the chromogen (3’-diaminobenzidine/DAB) used produces brown ‘positive’ staining. However, the frequent presence in the tumours of melanin pigment (brown to black colour in sections from FFPE tissue) could have effectively decreased the sensitivity with which positive lymphatic vessels could

be detected (low contrast between positive IHC signal and melanin pigment), even if a clear distinction between IHC signal and melanin in regard to sub-cellular localisation is possible as Prox-1 positive signal is present in the nucleus of endothelial cells and melanin is localised in the cytoplasm of melanomas cells. Another potential issue that would have resulted in a lower rate of lymphatic invasion detection is the difficult delineation of the cellular borders of endothelial cells in IHC-stained sections compared to those visualised in H&E-stained sections (as just said, Prox-1 IHC gives only a positive nuclear signal). Consequently, it was sometimes challenging to determine if lymphatic vessels were collapsed due to compression by melanoma cells, or if the vascular lumen was completely filled with neoplastic cells, despite the detection of positive nuclei of endothelial cells in the area. Future projects could try to use other lymphatic-specific markers (e.g. LYVE-1, which gives a cytoplastic positive signal) and an alternative chromogen (e.g. 3-Amino-9-Ethylcarbazole/*AEC,* which is a red chromogen) to try to solve these potential issues and improve the sensitivity of the assay.

Interestingly, the study showed that the sensitivity of detecting lymphatic invasion could be increased by evaluating peritumoural (PT) areas, instead of intratumoural (IT) areas in canine primary OMMs. In human medicine there has been a long debate regarding the biological and clinical roles of intratumoural lymphatic vessels. Some studies have shown that a relatively high incidence of IT LVI correlates with adverse clinical outcome and with sentinel lymph nodal metastasis, whereas others have reported that LVI is more common, or is only detected in the PT area[14]. Moreover, functional studies of xenograft mice have suggested that IT lymphatic vessels are not functional and that the ones at the tumour margins are solely responsible for the metastatic dissemination[103]. Therefore, one can hypothesise that canine OMMs may preferentially use PT lymphatic vessels to disseminate to distant organs.

Assessment of the correlation between presence of lymphatic invasion in the primary tumour and lymph nodal metastasis was performed. Our results showed that evaluation of lymphatic invasion in canine primary OMMs seems to results in potential high numbers of false negatives (low sensitivity) and low numbers of false positives (high specificity) in predicting lymph node metastasis.

Thinking about the strong functional and anatomical correlation between the lymphatic vessels and the regional/draining lymph nodes, one would assume that the presence of lymphatic invasion in the primary site always/frequently matches lymph nodal

metastasis, or at least that lymphatic invasion in the primary site would occur more often than lymph nodal metastasis because not all neoplastic cells entering the lymphatic system are able to reach the lymph node. However, this assumption has been proven to be wrong as the reported incidence of LVI is disproportionately low compared to the incidence of sentinel lymph node positivity on routine histologic evaluation, for example in human cutaneous melanomas[19]. Similar results have also been reported from another study on human melanomas, where 75% of primary tumours with lymphatic invasion had metastatic lymph nodal metastasis and 31% of primary tumours without lymphatic invasion had metastatic lymph nodal metastasis[19]. The presence of lymphovascular invasion also showed a weak correlation with the occurrence of lymph nodal metastasis in human breast cancer[16].

Although lymphatic invasion is an early event in the metastatic process, it seems that it is a better predictor of the ultimate outcome of the disease rather than of a more immediate event such as sentinel/regional lymph node metastasis[14]. For the same reason, we can hypothesise that the spreading of melanoma cells from the primary site to the lymph node possibly took place early in the development of the tumour and therefore there is lower incidence of lymphatic invasion in the primary site at the time of excision.

However, we have to bear in mind that assessment of LVI is variable between pathologists, depending on several factors. Only fair agreement among six pathologists in the evaluation of LVI in human colorectal cancer has been reported by Harris et al[104]. Rakha et al have shown that a high level of consistency of reporting LVI is possible in human breast cancer, however only with high numbers of involved lymphovascular spaces in the examined sections[105]. Beggan et al showed that variation of interobserver agreement in the diagnosis of LVI in human squamous cell carcinoma of the floor of the mouth can be substantial[106]. Interestingly, they pointed out that interpretative variation seems to be the main factor contributing to discrepant diagnoses. Our results can support the hypothesis that the same is true for the agreement in detecting lymphatic invasion in canine primary OMMs. Indeed, the agreement between our group of three pathologists was quite variable, despite we have tried to reduce presence of other factors potentially influencing observers' concordance. For example, all three pathologists examined the same sections (H&E and Prox-1 IHC-stained sections), therefore not incurring in the possible variation of the tissue in different levels of each FFPE tissue block. We have also defined the specific features of "lymphatic invasion"

for our study before starting the examination (see Materials and methods), limiting the variability in the criteria used to recognize and define lymphatic invasion by each pathologist.

Therefore, future studies should aim to increase both the detection of lymphatic invasion and the agreement between pathologists to obtain more reliable data on the clinical and biological significance of lymphatic invasion in cancer.

Limitations of the study:

The main limitation of this study was the relatively low numbers of metastatic and non-metastatic OMMs evaluated. Due to high frequency of nodal metastasis at presentation, identification of non-metastatic cases can be challenging, and representative and comparable cohorts of both metastatic and non-metastatic OMMs are required to obtain reliable results. Therefore, in a future study to number of cases would be expanded, and follow-up data on the occurrence of distant metastases potentially availed to try to test the hypothesis of the prognostic significance of lymphatic invasion, and evaluate the potential important role of peritumoural lymphatics in tumour metastasis. As previously discussed, adjustment of the IHC protocol may increase the detection of lymphatic vessels, and the reliability of other IHC markers for lymphatic vessel detection in canine OMMs could be investigated.

Future work:

In collaboration with Dr. McConnel, Research Associate from Dermatological Sciences, Institute of Cellular Medicine, Newcastle University, we are trying to investigate the potential use of IHC markers as prognostic factors in canine melanomas (oral and cutaneous). In particular, AMBRA1 (Autophagy And Beclin 1 Regulator 1) has been already shown to be predictive in term of prognosis for early stage human melanomas (Epidermal autophagy and beclin 1 regulator 1 and loricrin: a paradigm shift in the prognostication and stratification of the American Joint Committee on Cancer stage I melanomas. Ellis R et al. Br J Dermatol. 2019 May 6. doi: 10.1111/bjd.18086. [Epub ahead of print]). We already tried to investigate the expression of AMBRA1 in canine tissues (skin and oral mucosa), with promising results. Our aim for the next few months is to set up a scoring system for the evaluation of AMBRA1 in canine FFPE OMM samples and expand the cohort of cutaneous melanoma in collaboration with Dr

Brachelente, Associate Professor, Department of Veterinary Medicine, Perugia University.

Scientific activity carried out during the PhD:

My scientific activity has taken place mainly at the Department of Pathology and at the Department of Molecular Oncology of the Animal Health Trust (United Kingdom), under close supervision of Dr. Mike Starkey (Head of Molecular Oncology) and distant supervision of Prof. Brunetti Barbara from the Department of Veterinary Medical Science of *Alma Mater Studiorum*-Bologna University. The PhD project focused on canine oral malignant melanomas, in particular on several genomic and immunohistochemical features which could be used in the future for prognostic purposes.

During these three years, I had the opportunity to increase my knowledge on different genomic approaches to investigate variation in gene expression between canine primary oral mucosal melanomas and their matched lymph nodal metastases. I have been involved in the study plan since the beginning, trying to adjust the project according to the time, funding and material available. I have been in the lab to do myself several experiments, under the supervision of Dr. Starkey. Internal (Animal Health Trust as Collaborator) and external (Petplan Charitable Trust-Pump Priming Grant as Primary Investigator) funding have been obtained to support the project. Currently, I am waiting for the decision upon application for funding to the American Kennel Club Canine Health Foundation-Acorn Grant as Co-Primary Investigator (together with Dr. Starkey) to be able to perform RNA-sequence analysis, quantitative RT-PCR and Sanger DNA sequencing in the collected canine oral malignant melanoma samples.

Internal (Animal Health Trust as Principal Investigator) funds have been awarded to support the Prox-1 immunohistochemical study on canine primary oral melanomas.

During my PhD, I have been working at the Animal Health Trust as Anatomic pathologist and for 6 months as Acting Head of Anatomic pathology, being responsible for the biopsy and necropsy services. I have been training with rounds and seminars on anatomic pathology Interns and Residents in different disciplines during these years and I have been the supervisor of an Intern in Anatomic pathology for 8 months. I have also been co-supervisor of a visiting PhD student for 4 months.

Publications during the PhD:

- Inter- and Intraobserver Agreement of Canine and Feline Nervous System Tumors. Belluco S, Avallone G, Di Palma S, Rasotto R, Oevermann A. Veterinary Pathology. 2019 May;5(3):342-349.
- Identification of molecular genetic contributants to canine cutaneous mast cell tumour metastasis by global gene expression analysis. Bowlt Blacklock K, Birand Z, Biasoli D, Fineberg E, Murphy S, Flack D, Bass J, Di Palma S, Blackwood L, McKay J, Whitbread T, Fox R, Eve T, Beaver S, Starkey M. PLoS One. 2018 Dec 19;13(12):e0208026.
- Meningeal carcinomatosis secondary to a suspected pulmonary carcinoma in a cat and comparison with human literature. Crespo V, Ortega M, Stabile F, Di Palma S, Fernandez Y. Veterinary Record Case Reports. 2018; 6(4).
- Recurrent cerebrovascular accidents caused by intravascular lymphoma in a dog. Sanchez L, Beckmann K, Dominguez E, Di Palma S, Shea A. Veterinary Record Case Reports. 2018;6(3).
- Spontaneous gall bladder infarction in a dog with a congenital extrahepatic portosystemic shunt. Olivares G, Fernandez Y, Di Palma S, Murgia D. Veterinary Record Case Reports. 2018;6(1).

Poster during the PhD:

- Lymphatic invasion in canine oral melanoma: can the sensitivity of detection be increased by Prox-1 immunohistochemistry? Pellegrino V, Avallone G, Brunetti B, Di Palma S. Annual Meeting ESVP/ECVP, 25-28 September 2019, Arnhem (The Netherlands).

LYMPHATIC INVASION IN CANINE ORAL MELANOMA: CAN THE SENSITIVITY OF DETECTION BE INCREASED BY PROX-1 IMMUNOHISTOCHEMISTRY?

V. Pellegrino*, G. Avallone*, B. Brunetti*, S. Di Palma *†
*Department of Veterinary Medical Sciences (DIMEVET), University of Bologna, Italy;
† Animal Health Trust, Newmarket, UK and, current affiliation, Aptuit (Verona) Srl, an Evotec Company

INTRODUCTION

Malignant melanoma is the most common canine oral cancer and frequently metastasizes to draining lymph nodes. Histological identification of neoplastic emboli has been reported to be a predictor of metastatic dissemination.

AIM

To evaluate the potentially increased sensitivity and specificity in the detection of lymphatics neoplastic emboli using PROX-1 (immunohistochemical marker for lymphatic vessels).

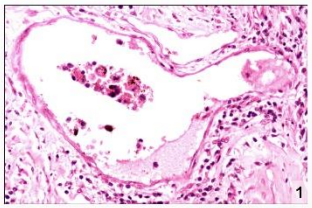
1

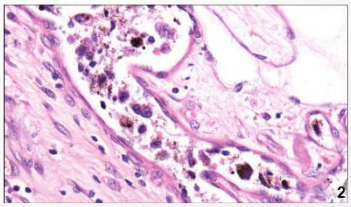
2

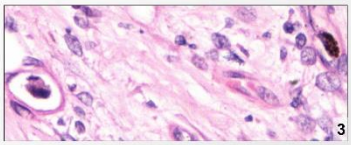
3

Images 1,2,3: oral malignant melanomas, H&E stain: suspected lymphatic intratumoral neoplastic embolus.

MATERIALS AND METHODS

Thirty-six histologic sections from 21 primary canine oral melanomas, for which the metastatic status of the draining lymph nodes was known, have been blindly evaluated by three pathologists for the presence/absence of lymphatic invasion on H&E stained and PROX-1 IHC stained sections. Statistical analysis was performed to assess the inter-pathologist agreement and the specificity/ sensitivity of the evaluation of HE and PROX1 stained sections to predict the metastatic status of the draining lymph-node.

RESULTS

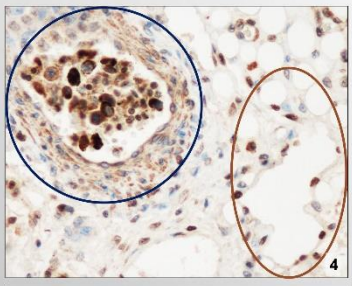
4

Image 4: Prox-1 IHC, DAB chromogen: oral malignant melanomas: on the left: negative endothelial cells to Prox-1 in a vessel containing neoplastic cells (hematic embolus); on the right strong nuclear labelling of lymphatic endothelial cells lining lymphatic vessels whitout neoplastic cells.

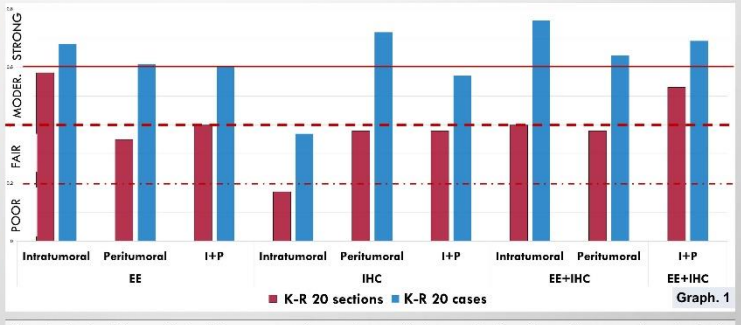

Graph. 1

Graph. 1: the inter-pathologist agreement was always higher evaluating the entire case (moderate to strong) rather than single sections (fair to moderate). The average sensitivity did not exceed 50% and was lower when evaluating intratumoral emboli. The specificity was always higher than sensibility and was reduced when assessing intratumoral emboli.

CONCLUSIONS

Based on these results:

- The inter-pathologist agreement can be increased by the evaluation of multiple section from the same tumor.
- The optimal combination of sensibility and specificity is obtained by evaluation of peritumoral tissue on H&E stained section.
- Prox-1 immunohistochemistry does not seem to be a useful tool to detect lymphatic neoplastic emboli.

Munday JS, Lohr CV, Kiupel M; Tumors of the alimentary tract in Tumors in Domestic Animals, Fifth Edition, ed. DJ Meuten, 2017.
Smedley RC, Lamoureux J, Sledge DG, Kiupel M. Immunohistochemical diagnosis of canine oral amelanotic melanocytic neoplasms. Vet Pathol. 2011 Jan;49(1):32-40.
Esplin DG. Survival of dogs following surgical excision of histologically well-differentiated melanocytic neoplasms of the mucous membranes of the lips and oral cavity. Vet Pathol. 2008 Nov;45(6):889-96.
Uzal FA, Plattner BL, Hostetter JM Alimentary system in Jubb, Kennedy & Palmer's Pathology of Domestic Animals (Fifth Edition), Vol2, Edited by M. Grant Maxie Elsevier, 2017, 26-27.
Smedley RC, Spangler WL, Esplin DG, Kitchell BE, Bergman PJ, Ho HY, Borgin IL, Kiupel M. Prognostic markers for canine melanocytic neoplasms: a comparative review of the literature and goals for future investigation. Vet Pathol. 2011 Jan;48(1):54-72.
Rose AE, Christos P J, Lackaye D, Shapiro RL, Berman R, Mazumdar M, Kamino H, Osman I, Darvishian F. Clinical relevance of detection of lymphovascular invasion in primary melanoma using endothelial markers D2-40 and CD34. Am J Surg Pathol. 2011 Oct;35(10):1441-9.
Guiam FJ, Going JJ, Mohammed ZM, Orange C, Edwards J, McMillan DC. Immunohistochemical detection improves the prognostic value of lymphatic and blood vessel invasion in primary ductal breast cancer. BMC Cancer. 2014 Sep 18;14:676.
Alexander-Sefre F, Singh N, Ayhan A, Salvesen HB, Wilbanks G, Jacobs IJ. Detection of tumour lymphovascular space invasion using dual cytokeratin and CD31 immunohistochemistry. J Clin Pathol. 2003 Oct;56(10):786-8.

ESVP-ECVP ANNUAL MEETING 2019 - SEPTEMBER 25TH – 28TH, 2019, ARNHEM, THE NETHERLANDS

Appendix 1

RNA extraction using the RecoverAll Total Nucleic Acid Isolation Kit:

1. Transfer 3 tissue cores extracted from the highlighted areas of the FFPE block using a Miltex Biopsy punch with plunger into a Nuclease-free 2ml Eppendorf tube.
2. Add 1.8ml of Histoclear to submerge the cores. Incubate at 37°C for 1 hour on a rotary mixer.
3. Centrifuge at 13,000 rpm for 10 minutes at room temperature to pellet the tissue. Carefully remove the Histoclear.
4. Add 1ml of 100% ethanol and mix by vortexing. Centrifuge at 13,000 rpm for 2 minutes at room temperature to pellet the tissue. Carefully remove the ethanol-Histoclear.
5. Add 1ml of 100% ethanol and mix by vortexing. Centrifuge at 13,000 rpm for 2 minutes at room temperature to pellet the tissue. Carefully remove as much the ethanol-Histoclear as possible.
6. Add 1ml of 10% Phosphate-buffered saline/PBS (pH 7.2) and mix by vortexing. Centrifuge at 13,000 rpm for 2 minutes at room temperature to pellet the tissue. Carefully remove the PBS-Histoclear.
7. Add 1ml of 10% PBS (pH 7.2) and mix by vortexing. Centrifuge at 13,000 rpm for 5 minutes at room temperature to pellet the tissue. Carefully remove the PBS-Histoclear.
8. Allow the tissue pellet to air dry for 1 hour.
9. Add 400µl of Digestion Buffer and 8µl of Protease.
10. Swirl gently to mix and to immerse the tissue. Briefly centrifuge to bring the tissue down into the solution.
11. Incubate in a waterbath at 50°C for 3 hours.
12. Transfer a 200µl aliquot into a 2ml Nuclease-free Eppendorf tube.
13. Incubate the 200µl aliquot at 80°C for 15 minutes.
14. Add 240µl of Isolation Additive and mix by vortexing. Add 550µl of 100% ethanol and mix by pipetting.
15. Centrifuge at 10,200 rpm for 10 seconds at room temperature.
16. Pipette 700µl of the ~994µl sample/ethanol mixture onto a Filter Cartridge placed inside a Collection Tube.

17. Centrifuge at 10,200 rpm for 60 seconds to pass the mixture through the filter. Discard the flow-through, and re-insert the Filter Cartridge in the same Collection Tube.
18. Repeat steps 16. and 17. once more until all of the ~994µl sample/ethanol mixture has passed through the filter. Discard the flow-through on each occasion.
19. Add 700µl of Wash 1 (to which ethanol was previously added) to the Filter Cartridge. Centrifuge at 10,200 rpm for 30 seconds to pass the mixture through the filter. Discard the flow-through, and re-insert the Filter Cartridge in the same Collection Tube.
20. Add 500µl of Wash 2/3 (to which ethanol was previously added) to the Filter Cartridge. Centrifuge at 10,200 rpm for 30 seconds to pass the mixture through the filter. Discard the flow-through, and re-insert the Filter Cartridge in the same Collection Tube. Centrifuge at 10,200 rpm for 30 seconds to remove residual fluid from the filter.
21. On ice, combine 50µl of Nuclease-free water, 6µl of 10 x DNase Buffer and 4µl of DNase. Carefully add the 60µl of DNase mix to the centre of the Filter Cartridge and incubate at 37°C for 30 minutes.
22. Add 500µl of Wash 2/3 (to which ethanol was previously added) to the Filter Cartridge. Centrifuge at 10,200 rpm for 30 seconds to pass the mixture through the filter. Discard the flow-through, and re-insert the Filter Cartridge in the same Collection Tube.
23. Repeat step 22. with a second 500µl of Wash 2/3, and re-insert the Filter Cartridge in the same Collection Tube. Centrifuge at 10,200 rpm for 1 minute to remove residual fluid from the filter.
24. Transfer the Filter Cartridge to a fresh Collection Tube, and carefully apply 30µl of Nuclease-free water to the centre of the filter. Incubate at room temperature for 1 minute. Centrifuge at 13,000 rpm for 1 minute to elute RNA.
25. Repeat step 24 with a second 30µl of Nuclease-free water, using the same Collection Tube.
26. Transfer the ~60µl of total RNA to a labelled Nuclease-free 1.5ml Eppendorf tube.

Appendix 2

RNA samples purification by spin column filtration:

1. Zymo-Spin IV-HRC Columns need to be prepared prior to use by:
   1.1. Snapping off the base
   1.2. Removing the cap
   1.3. Inserting into a Collection Tube
   1.4. Spinning in a microcentrifuge at 8,000 x g for 3 minutes
2. Transfer 55-58µl RNA to a prepared Zymo-Spin IV-HRC in a clean 1.5ml microcentrifuge tube.
3. Centrifuge at 8,000 x g for 1 minute.

Appendix 3

Measurement of total RNA concentration using the NanoDrop spectrophotometer:

1. Pipette 2µl of total RNA for each sample onto the lower measurement pedestal.
2. Close the sampling arm and initiate a spectral measurement using the operating software on the PC.
3. When the measurement is complete, open the sampling arm and wipe the sample from both the upper and lower pedestal using a soft laboratory wipe.
4. Record the value obtained from the measurement.
5. Pipette 2µl of water aliquots to clean the measurements surfaces and then wipe the surfaces with a soft laboratory wipe.
6. Proceed with the next measurement of RNA sample.

Appendix 4

Measurement of total RNA concentration using the Quant-iT RiboGreen assay:

1. Prepare 50ml of 10mM Tris-HCl (pH 7.5), 1mM EDTA by diluting 2.5ml of 200mM Tris-HCl, 20 mM EDTA in 47.5ml of Nuclease-free water.
2. Dilute 1µl of each RNA sample (previously quantified by UV spectrophotometry) in a volume of 10mM Tris-HCl, 1mM EDTA that yielded a concentration of 900ng/ml.
3. Prepare 5x “high range E. coli 16S and 23S rRNA standars” to obtain final RNA concentration in assay of 1 µg/ml, 500 ng/ml, 100 ng/ml, 20 ng/ml and 0 ng/ml.
4. Prepare 33µl of 1x RiboGreen reagent in 10mM Tris-HCl, 1mM EDTA for every RNA sample by diluting stock RiboGreen reagent 200-fold in 10mM Tris-HCl, 1mM EDTA.
5. Combine 10µl of RNA and 10µl of 1x RiboGreen reagent in each of 3 x 0.2ml PCR tubes. For each of the triplicate 0 ng/ml rRNA standard assay, add 10µl of 10mM Tris-HCl, 1mM EDTA to 10µl of 1x RiboGreen reagent. Perform 3x assays for each RNA sample and rRNA standard. Seal the 96-well plate with a MicroAmp Otpical Adhesive. Store in the dark for 2-5 minutes.
6. Centrifuge the PCR plate at 1000 rpm for 1 minute.
7. Measure the fluorescence of each sample using the ABI StepOnePlus PCR machine (5 cycles of 20°C for 10 seconds).
8. For each PCR plate well that contains a RNA sample (including the 0ng/ml rRNA standard), calculate the median of RiboGreen fluorescence signal intensity from the value obtained for each well in each of the 5 cycles.
9. For each RNA sample, calculate the median RiboGreen fluorescence signal intensity from the median values calculated for each of the 3 replicate PCR plate wells.

Appendix 5

Preparation of biotin-labelled single-stranded-cDNA for hybridisation to a Canine Gene 1.1 ST Array Strip

1. Tumour RNA sample preparation
   1.1. Adjust the RNA concentration of each sample to obtain 3µl of RNA solution containing approximately 29ng/µl of RNA.
2. First strand cDNA synthesis and excess primer removal
   2.1. On ice, combine 3µl (≥2ng) of each RNA sample with 2µl of Poly-A Control RNA Dilution 4 in a RNase-free 1.5ml Eppendorf tube.
   2.2. Add 5µl of First-Strand Master Mix to each. Mix thoroughly by gentle vortexing. Briefly centrifuge and place on ice. Transfer each into a PCR microtitre plate well. Briefly centrifuge and place on ice.
   2.3. In a PCR machine (Heated lid set at 42°C), incubate at 25°C for 5 min, 42°C for 60 min and 4°C for 5 min. Briefly centrifuge.
   2.4. Place the microtite plate on ice, and after 2 min, add 2µl of WT Pico Cleanup Reagent to each First-Strand cDNA Synthesis Mix. Mix gently by pipetting and ensure that all the liquid has been expelled from the pipette tip. Briefly centrifuge and place back on ice.
   2.5. In a PCR machine (Heated lid set at 105°C), incubate at 37°C for 30 min, 80°C for 10 min, and 4°C for 5 min. Briefly centrifuge and place the microtitre plate on ice.
   2.6. Start a 15°C, 'forever' run on the PCR machine block that will be used for the '3' Adaptor synthesis' reactions.
3. 3` Adaptors synthesis
   3.1. On ice, add 8µl of 3' Adaptor Master Mix to each 12µl first strand cDNA sample. Mix gently by pipetting up and down. Briefly centrifuge and place back on ice.
   3.2. In a PCR machine (Heated lid turned off), incubate at 15°C for 15 min, 35°C for 15 min, 70°C for 10 min and 4°C for 5 min. Briefly centrifuge (4,000 rpm, 1 min) and place the microtitre plate on ice.
4. Pre-In Vitro Transcription (IVT) ds-cDNA PCR amplification
   4.1. On ice, add 30µl of Pre-IVT Amplification Master Mix to each 20µl adaptored first strand cDNA sample. Mix gently by pipetting up and down. Briefly centrifuge and place back on ice.

4.2. In a PCR machine (Heated lid set at 105°C), incubate at 95°C for 2 min, followed by 12 cycles of (94°C for 30s, 70°C for 5 min), and 4°C for 5 min. Briefly centrifuge and place the microtitre plate on ice.

5. In Vitro Transcription

5.1. Incubate the microtitre plate containing the ds-cDNA samples at room temperature for 5 min.

5.2. To each 50µl cDNA sample, add 30µl of IVT Master Mix. Mix gently by pipetting up and down. Centrifuge briefly.

5.3. In a PCR machine (Heated lid set at 40 or 50°C), incubate at 40°C for 16h, and 4°C 'forever'. Briefly centrifuge

6. Purification of cRNA

6.1. Shake/vortex the Purification beads to resuspend the beads. Dispense 154µl of Purification beads per cRNA sample into an RNAse-free 2ml Eppendorf tube. Store at room temperature.

6.2. Place 2 x 1ml tubes of Nuclease-free water in the 65°C Hybridisation Oven.

6.3. Prepare 7ml of 80% (v/v) ethanol.

6.4. For each sense RNA sample, aliquot 140µl of purification beads into 1 well of a round bottom 96-well microtitre plate. Store at room temperature.

6.5. Add a 80µl cRNA sample to each microtitre plate well. Mix gently by pipetting up and down.

6.6. Incubate at room temperature (20-25°C) for 10 min.

6.7. Place the microtitre plate on a magnetic stand for 10 min to separate the beads from the solution.

6.8. Slowly remove (and discard) the ~220µl solution, taking care not to disturb the purification beads.

6.9. Whilst on the magnetic stand, add 200µl of 80% (v/v) ethanol to each well. Incubate at room temperature for 30s.

6.10. Slowly remove the 80% (v/v) ethanol taking care not to disturb the purification beads.

6.11. Repeat steps 9. and 10. twice more. Completely remove the 80% (v/v) ethanol.

6.12. Allow the beads to air-dry on the magnetic stand for at least 5 min until no liquid is visible and yet the bead pellets appear shiny.

6.13. Remove the microtitre plate from the magnetic stand, and add 27µl of the 65°C Nuclease-free water to each well.

6.14. Once water has been added to all the wells, incubate at room temperature for 3 min, pipetting the beads up and down to resuspend.

6.15. Place the microtitre plate on the magnetic stand for 5 min to separate the beads from the solution.

6.16. Carefully aspirate each cRNA sample into a RNase-free 1.5ml Eppendorf tube (placed on ice). Record the volume recovered.

6.17. Measure the concentration and 'purity' of a 1µl aliquot (diluted with 1µl of Nuclease-free water) of each cRNA sample using the NanoDrop.

6.18. Store at -20°C overnight OR at -70°C long-term.

7. Single-stranded cDNA synthesis

7.1. On ice, dispense each 24µl (=20µg) cRNA sample into a RNase-free 1.5ml Eppendorf tube.

7.2. Add 16µl of 2nd-Cycle ss-cDNA Master Mix to each. Mix gently by tube flicking. Briefly centrifuge and place on ice. Transfer each into a PCR microtitre plate well.

7.3. In a PCR machine (Heated lid set at 70°C), incubate at 25°C for 10 min, 42°C for 90 min, 70°C for 10 min, and 4°C 'forever'. Briefly centrifuge.

8. RNA removal

8.1. On ice, add 4µl of RNase H to each 40µl 2nd-Cycle ss-cDNA sample. Mix gently by pipetting up and down twice. Centrifuge briefly. Place back on ice.

8.2. In a PCR machine (Heated lid set at 105°C), incubate at 37°C for 45 min, 95°C for 5 min, and 4°C 'forever'. Briefly centrifuge and place on ice.

8.3. Add 11µl of Nuclease-free water to each 44µl ss-cDNA sample. Mix gently by pipetting up and down twice. Centrifuge briefly. Place back on ice.

9. Purification of ss-cDNA

9.1. Shake/vortex the Purification beads to resuspend the beads. Dispense 110µl of Purification beads per ss-cDNA sample into an RNAse-free 2ml Eppendorf tube. Store at room temperature.

9.2. Place 3 x 1ml tubes of Nuclease-free water in the 65°C Hybridisation Oven.

9.3. Prepare 7ml of 80% (v/v) ethanol.

9.4. For each ss-cDNA sample, aliquot 100µl of purification beads into 1 well of a round bottom 96-well microtitre plate. Store at room temperature.

9.5. Add a 55µl ss-cDNA sample to each microtitre plate well. Mix gently by pipetting up and down.

9.6. Add 150µl of 100% (v/v) ethanol to each sample. Mix gently by pipetting up and down.

9.7. Incubate at room temperature (20-25°C) for 20 min.

9.8. Place the microtitre plate on a magnetic stand for 10 min to separate the beads from the solution.

9.9. Slowly remove (and discard) the ~305µl solution, taking care not to disturb the purification beads.

9.10. Whilst on the magnetic stand, add 200µl of 80% (v/v) ethanol to each well. Incubate at room temperature for 30s.

9.11. Slowly remove the 80% (v/v) ethanol taking care not to disturb the purification beads.

9.12. Repeat steps 10. and 11. twice more. Completely remove the 80% (v/v) ethanol.

9.13. Allow the beads to air-dry on the magnetic stand for at least 5 min until no liquid is visible and yet the bead pellets appear shiny.

9.14. Remove the microtitre plate from the magnetic stand, and add 30µl of the 65°C Nuclease-free water to each well.

9.15. Once water has been added to all the wells, incubate at room temperature for 3 min, pipetting the beads up and down to resuspend.

9.16. Place the microtitre plate on the magnetic stand for 5 min to separate the beads from the solution.

9.17. Carefully aspirate each ss-cDNA sample into a RNase-free 1.5ml Eppendorf tube (placed on ice). Record the volume recovered.

9.18. Measure the concentration and 'purity' of a 1µl aliquot (diluted with 1µl of Nuclease-free water) of each ss-cDNA sample using the NanoDrop.

9.19. Store at -20°C overnight OR at -70°C long-term.

10. <u>Fragmentation and labelling of single-stranded cDNA</u>

10.1. On ice, dispense each 46µl Single-Stranded cDNA sample into a RNase-free 1.5ml Eppendorf tube.

10.2. Add 14µl of Fragmentation and Labelling Master Mix to each. Mix thoroughly by gentle vortexing. Briefly centrifuge and place on ice. Transfer each into a PCR microtitre plate well.

10.3. In a PCR machine (Heated lid set at 93°C), incubate at 37°C for 60 min, 93°C for 2 min, and 4°C `forever`. Briefly centrifuge.

10.4. Transfer each 60µl fragmented and labelled Single-Stranded cDNA sample to a RNase-free 1.5ml Eppendorf tube.

11. Hybridization cocktail preparation

11.1. For each ss-cDNA sample, at room temperature, in a RNase-free 1.5ml Eppendorf tube combine:

11.1.1. Hybridisation Master Mix (49µl per sample)

11.1.2. Fragmented and labelled Single-Stranded cDNA (41µl per sample)

11.1.3. 2.5 x WT Hyb Add 6 (60µl per sample)

GeneChip WT Pico Reagent Kit work flow:

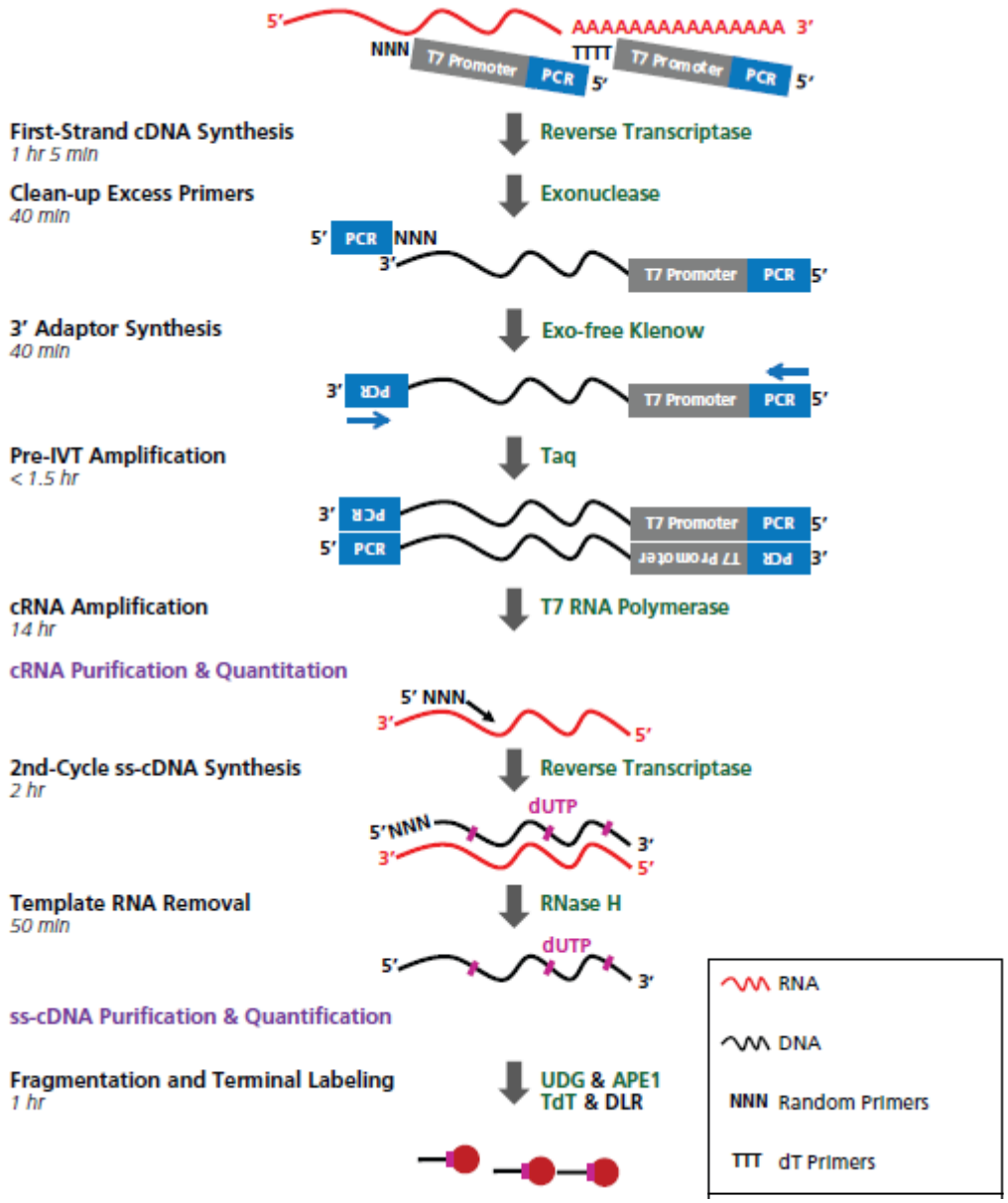

Appendix 6

Immunohistochemistry for PROX-1:

1. A 3-µm thick section is obtained from each case and mounted on a pre-cleaned X-tra Adhesive slide (Leica Biosystems).
2. Slides are left in the oven overnight at 45-50°C.
3. Place overnight dried slides into Dako PT Link for antigen retrieval (EnVision FLEX Target Retrieval Solution, Low pH/ citrate buffer pH 6.1).
   3.1. Fill PT Link with sufficient quantity of working solution to cover the tissue sections.
   3.2. Set PT link to pre-heat the solution at 65°C
   3.3. Immerse the tissue sections into the pre-heated Target Retrieval Solution and incubate for 30 minutes at 97°C.
   3.4. Leave the sections to cool in PT Link to 65°C.
   3.5. Remove the slides from the PT Link and dip them into a jar with diluted Dako Wash Buffer at room temperature.
   3.6. Leave slides for 5 minutes.
4. Put slides in Dako Autostainer Plus Link to perform immunohistochemistry run with the following program.
   4.1. Dako Wash Buffer: 0 minutes
   4.2. Envision Flex Peroxidase Block Reagent (Dako): 5 minutes
   4.3. Dako Wash Buffer: 0 minutes
   4.4. Prox-1 antibody (dilution 1:500): 20 minutes
   4.5. Dako EnVision+ System – HRP (Dako): 30 minutes
   4.6. Dako Wash Buffer: 5 minutes
   4.7. DAB + Substrate Chromogen System (Dako): 10 minutes
   4.8. Dako Wash Buffer: 0 minutes
   4.9. Haematoxylin: 5 minutes
   4.10. Rinse deionized Water: 0 minutes
   4.11. Dako Wash Buffer: 5 minutes
   4.12. Rinse deionized Water: 0 minutes
5. Dehydrate tissue sections.
   5.1. 3 changes of 95% ethanol for 1-2 minutes each
   5.2. 2 changes of 100% ethanol for 1-2 minutes each
   5.3. 3 changes of Xylene for 1 minute each

6. Coverslip tissue sections.

Acknowledgment:

I would first like to thank my thesis supervisor, Associate Professor Barbara Brunetti of the Department of Veterinary Medical Sciences at the University of Bologna. She gave me the invaluable opportunity to dedicate part of my life to research.
I cannot find words to express my gratitude to Dr Mike Starkey, Head of Molecular Oncology at the Animal Health Trust (UK). He has been my mentor throughout the entire project. His guidance helped me in all the difficult times of research and writing of this thesis. I could not have imagined having a better advisor for my PhD study.

I would also like to thank all the other great collaborators of the project:

- Dr Willie Bergmann, Dr Elena Riccardi, Dr Fabio Aloisio and Dr Kelly Bowlt Blacklock for sharing precious material to be included in the experiments.
- Deborah Biasoli for helping me in the Molecular Oncology lab at the Animal Health Trust.
- Dr Giancarlo Avallone and Dr Valeria Pellegrino for their contribution in the histological examination of canine oral malignant melanoma cases.

My sincere thanks also go to all the members of the Pathology Department at the Animal Health Trust, who supported me in this great adventure.

Finally, this thesis would not have been possible without the daily support of my wife and the joy of my daughter. Their presence has been the reason for me to keep going despite several hiccups in these three years and finish this great achievement.

Bibliography

1. Mort, R. L., Jackson, I. J. & Elizabeth Patton, E. The melanocyte lineage in development and disease. *Dev.* 142, 620–632 (2015).

2. Tief, K., Hahne, M., Schmidt, A. & Beermann, F. Tyosinase, the key enzyme in melanin synthesis, is expressed in murine brain. *Eur. J. Biochem.* 241, 12–16 (1996).

3. Kobayashi, N. *et al.* Supranuclear melanin caps reduce ultraviolet induced DNA photoproducts in human epidermis. *J. Invest. Dermatol.* 110, 806–810 (1998).

4. Feller, L. *et al.* Melanin: The biophysiology of oral melanocytes and physiological oral pigmentation. *Head Face Med.* 10, 1–7 (2014).

5. Guth, A. M. & Dow, S. *Withrow and MacEwen's Small Animal Clinical Oncology*. *Withrow and MacEwen's Small Animal Clinical Oncology, 5/e* (Elsevier, 2013). doi:10.1016/B978-1-4377-2362-5.00013-X

6. Munday, J. S., Löhr, C. V. & Kiupel, M. Tumors of the Alimentary Tract. in *Tumors in Domestic Animals* (John Wiley & Sons, Inc., 2016). doi:10.1002/9781119181200.ch13

7. Williams, M. D. & Tischler, A. S. Update from the 4th Edition of the World Health Organization Classification of Head and Neck Tumours: Paragangliomas. *Head Neck Pathol.* 11, 88–95 (2017).

8. Chan, R. C. L., Chan, J. Y. W. & Wei, W. I. Mucosal melanoma of the head and neck: 32-year experience in a tertiary referral hospital. *Laryngoscope* 122, 2749–2753 (2012).

9. Prouteau & André. Canine Melanomas as Models for Human Melanomas: Clinical, Histological, and Genetic Comparison. *Genes (Basel).* 10, 501 (2019).

10. Nishiya, A. T. *et al.* Comparative aspects of canine melanoma. *Vet. Sci.* 3, 1–22 (2016).

11. Gillard, M. *et al.* Naturally occurring melanomas in dogs as models for non-UV pathways of human melanomas. *Pigment Cell Melanoma Res.* 27, 90–102 (2014).

12. Wong, K. *et al.* Cross-species genomic landscape comparison of human mucosal melanoma with canine oral and equine melanoma. *Nat. Commun.* 10, (2019).

13. Simpson, R. M. *et al.* Sporadic naturally occurring melanoma in dogs as a preclinical model for human melanoma. *Pigment Cell Melanoma Res.* 27, 37–47 (2014).

14. Rose, A. E. *et al.* Clinical relevance of detection of lymphovascular invasion in primary melanoma using endothelial markers D2-40 and CD34. *Am. J. Surg. Pathol.* 35, 1441–1449 (2011).

15. Samejima, J. *et al.* Prognostic significance of blood and lymphatic vessel invasion in pathological stage IA lung adenocarcinoma in the 8th edition of the TNM classification. *Lung Cancer* 137, 144–148 (2019).

16. Zhang, S. *et al.* The relationship of lymphatic vessel density, lymphovascular invasion, and lymph node metastasis in breast cancer: A systematic review and meta-analysis. *Oncotarget* 8, 2863–2873 (2017).

17. Gao, S. *et al.* Retrospective evaluation of lymphatic and blood vessel invasion and Borrmann types in advanced proximal gastric cancer. *World J. Gastrointest. Oncol.* 11, 642–651 (2019).

18. Millanta, F. *et al.* Proliferation activity in oral and cutaneous canine melanocytic tumours: Correlation with histological parameters, location, and clinical behaviour. *Res. Vet. Sci.* 73, 45–51 (2002).

19. Doeden, K. *et al.* Lymphatic invasion in cutaneous melanoma is associated with sentinel lymph node metastasis. *J. Cutan. Pathol.* 36, 772–780 (2009).

20. Moy, A. P., Duncan, L. M. & Kraft, S. Lymphatic invasion and angiotropism in primary cutaneous melanoma. *Lab. Investig.* 97, 118–129 (2017).

21. Sleeckx, N. *et al.* Evaluation of Immunohistochemical Markers of Lymphatic and Blood Vessels in Canine Mammary Tumours. *J. Comp. Pathol.* 148, 307–317 (2013).

22. Wennogle, S. A., Priestnall, S. L., Suárez-Bonnet, A., Soontararak, S. & Webb, C. B. Lymphatic endothelial cell immunohistochemical markers for evaluation of

the intestinal lymphatic vasculature in dogs with chronic inflammatory enteropathy. *J. Vet. Intern. Med.* 1669–1676 (2019). doi:10.1111/jvim.15545

23. Halsey, C. H. C., Worley, D. R., Curran, K., Charles, J. B. & Ehrhart, E. J. The use of novel lymphatic endothelial cell-specific immunohistochemical markers to differentiate cutaneous angiosarcomas in dogs. *Vet. Comp. Oncol.* 14, 236–244 (2016).

24. Sleeckx, N. *et al.* Lymphangiogenesis in canine mammary tumours: A morphometric and prognostic study. *J. Comp. Pathol.* 150, 184–193 (2014).

25. Kawada, K. & Taketo, M. M. Significance and mechanism of lymph node metastasis in cancer progression. *Cancer Res.* 71, 1214–1218 (2011).

26. Wiley, H. E., Gonzalez, E. B., Maki, W., Wu, M. T. & Hwang, S. T. Expression of CC chemokine receptor-7 and regional lymph node metastasis of B16 murine melanoma. *J. Natl. Cancer Inst.* 93, 1638–1643 (2001).

27. Kawada, K. *et al.* Pivotal role of CXCR3 in melanoma cell metastasis to lymph nodes. *Cancer Res.* 64, 4010–4017 (2004).

28. Pereira, E. R. *et al.* Lymph node metastases can invade local blood vessels, exit the node, and colonize distant organs in mice. *Science (80-.).* 359, 1403–1407 (2018).

29. Smedley, R. C. *et al.* Prognostic markers for canine melanocytic neoplasms: A comparative review of the literature and goals for future investigation. *Veterinary Pathology* 48, 54–72 (2011).

30. Vinay Kumar, Abul K. Abbas, J. C. A. *Robbins and Cotran's Pathological Basis of Disease*. *Elsevier Health Sciences* (Elsevier/Saunders, [2015], 2014).

31. Sulaimon, S. S. & Kitchell, B. E. The Basic Biology of Malignant Melanoma: Molecular Mechanisms of Disease Progression and Comparative Aspects. *J. Vet. Intern. Med.* 17, 760–772 (2003).

32. Bowlt Blacklock, K. L. *et al.* Genome-wide analysis of canine oral malignant melanoma metastasis-associated gene expression. *Sci. Rep.* 9, 1–14 (2019).

33. Chiang, A. C. & Massagué, J. Molecular basis of metastasis. *New England*

Journal of Medicine (2008). doi:10.1056/NEJMra0805239

34. Hendrix, M. J. C. *et al.* Reprogramming metastatic tumour cells with embryonic microenvironments. *Nat. Rev. Cancer* 7, 246–255 (2007).

35. Trepat, X., Chen, Z. & Jacobson, K. Cell Migration. in *Comprehensive Physiology* (John Wiley & Sons, Inc., 2012). doi:10.1002/cphy.c110012

36. Schaks, M., Giannone, G. & Rottner, K. Actin dynamics in cell migration. *Essays Biochem.* 0, EBC20190015 (2019).

37. Suraneni, P. *et al.* The Arp2/3 complex is required for lamellipodia extension and directional fibroblast cell migration. *J. Cell Biol.* 197, 239–251 (2012).

38. Yamaguchi, H. *et al.* Molecular mechanisms of invadopodium formation: The role of the N-WASP-Arp2/3 complex pathway and cofilin. *J. Cell Biol.* 168, 441–452 (2005).

39. Rottner, K., Faix, J., Bogdan, S., Linder, S. & Kerkhoff, E. Actin assembly mechanisms at a glance. *J. Cell Sci.* 130, 3427–3435 (2017).

40. Murphy, D. A. *et al.* A Src-Tks5 pathway is required for neural crest cell migration during embryonic development. *PLoS One* 6, (2011).

41. Stetler-Stevenson, W. G. *et al.* Binding and Localization of Mr 72,000 Matrix Metalloproteinase at Cell Surface Invadopodia. *Cancer Res.* 53, 3159–3164 (1993).

42. Li, A. *et al.* Rac1 Drives Melanoblast Organization during Mouse Development by Orchestrating Pseudopod- Driven Motility and Cell-Cycle Progression. *Dev. Cell* (2011). doi:10.1016/j.devcel.2011.07.008

43. Ma, Y. *et al.* Fascin 1 is transiently expressed in mouse melanoblasts during development and promotes migration and proliferation. *Dev.* 140, 2203–2211 (2013).

44. Law, A. L. *et al.* Lamellipodin and the Scar/WAVE complex cooperate to promote cell migration in vivo. *J. Cell Biol.* 203, 673–689 (2013).

45. Yan, J. & Huang, Q. Genomics screens for metastasis genes. *Cancer Metastasis Rev.* 31, 419–428 (2012).

46. Birkeland, E. *et al.* Patterns of genomic evolution in advanced melanoma. *Nat. Commun.* 9, 1–12 (2018).

47. Furney, S. J. *et al.* Genome sequencing of mucosal melanomas reveals that they are driven by distinct mechanisms from cutaneous melanoma. *J. Pathol.* (2013). doi:10.1002/path.4204

48. Eisen, M. B., Spellman, P. T., Brown, P. O. & Botstein, D. Cluster analysis and display of genome-wide expression patterns. *Proc. Natl. Acad. Sci. U. S. A.* (1998). doi:10.1073/pnas.95.25.14863

49. Smyth, G. K. Linear models and empirical bayes methods for assessing differential expression in microarray experiments. *Stat. Appl. Genet. Mol. Biol.* (2004). doi:10.2202/1544-6115.1027

50. Hwa Yang, Y. & Speed, T. Design and analysis of comparative microarray experiments. in (2003). doi:10.1201/9780203011232.ch2

51. Camargo, A., Azuaje, F., Wang, H. & Zheng, H. Permutation - Based statistical tests for multiple hypotheses. *Source Code for Biology and Medicine* (2008). doi:10.1186/1751-0473-3-15

52. Huang, D. W., Sherman, B. T. & Lempicki, R. A. Systematic and integrative analysis of large gene lists using DAVID bioinformatics resources. *Nat. Protoc.* (2009). doi:10.1038/nprot.2008.211

53. Dennis, G. *et al.* DAVID: Database for Annotation, Visualization, and Integrated Discovery. *Genome Biol.* (2003). doi:10.1186/gb-2003-4-5-p3

54. Lin, K. T. *et al.* Vav3-Rac1 signaling regulates prostate cancer metastasis with elevated Vav3 expression correlating with prostate cancer progression and posttreatment recurrence. *Cancer Res.* (2012). doi:10.1158/0008-5472.CAN-11-2502

55. Terasawa, M. *et al.* Dimerization of DOCK2 Is Essential for DOCK2-Mediated Rac Activation and Lymphocyte Migration. *PLoS One* **7**, 1–7 (2012).

56. Sanui, T. *et al.* DOCK2 regulates Rac activation and cytoskeletal reorganization through interaction with ELMO1. *Blood* (2003). doi:10.1182/blood-2003-01-0173

57. Jiang, J., Liu, G., Miao, X., Hua, S. & Zhong, D. Overexpression of engulfment and cell motility 1 promotes cell invasion and migration of hepatocellular carcinoma. *Exp. Ther. Med.* 2, 505–511 (2011).

58. Dulak, A. M. *et al.* Exome and whole-genome sequencing of esophageal adenocarcinoma identifies recurrent driver events and mutational complexity. *Nat. Genet.* (2013). doi:10.1038/ng.2591

59. Castro-Castro, A. *et al.* Coronin 1A promotes a cytoskeletal-based feedback loop that facilitates Rac1 translocation and activation. *EMBO J.* (2011). doi:10.1038/emboj.2011.310

60. Nishiya, N., Kiosses, W. B., Han, J. & Ginsberg, M. H. An α4 integrin-paxillin-Arf-GAP complex restricts Rac activation to the leading edge of migrating cells. *Nat. Cell Biol.* 7, 343–352 (2005).

61. Pulkka, O. P. *et al.* Clinical relevance of integrin alpha 4 in gastrointestinal stromal tumours. *J. Cell. Mol. Med.* 22, 2220–2230 (2018).

62. Zlotnik, A. Chemokines in neoplastic progression. *Semin. Cancer Biol.* (2004). doi:10.1016/j.semcancer.2003.10.004

63. Zhao, Z. J. *et al.* CCL19-induced chemokine receptor 7 activates the phosphoinositide-3 kinase-mediated invasive pathway through Cdc42 in metastatic squamous cell carcinoma of the head and neck. *Oncol. Rep.* (2011). doi:10.3892/or.2010.1109

64. Illenberger, D., Walliser, C., Nürnberg, B., Lorente, M. D. & Gierschik, P. Specificity and structural requirements of phospholipase C-β stimulation by Rho GTPases versus G protein βγ dimers. *J. Biol. Chem.* 278, 3006–3014 (2003).

65. Favaro, P. *et al.* FMNL1 promotes proliferation and migration of leukemia cells. *J. Leukoc. Biol.* (2013). doi:10.1189/jlb.0113057

66. Denicourt, C., Saenz, C. C., Datnow, B., Cui, X. S. & Dowdy, S. F. Relocalized p27Kip1 tumor suppressor functions as a cytoplasmic metastatic oncogene in melanoma. *Cancer Res.* 67, 9238–9243 (2007).

67. Jeannot, P. *et al.* P27kip1 promotes invadopodia turnover and invasion through the regulation of the PAK1/cortactin pathway. *Elife* (2017).

doi:10.7554/eLife.22207

68. Pirone, D. M., Fukuhara, S., Gutkind, J. S. & Burbelo, P. D. SPECs, small binding proteins for Cdc42. *J. Biol. Chem.* 275, 22650–22656 (2000).

69. Podhajcer, O. L. *et al.* The role of the matricellular protein SPARC in the dynamic interaction between the tumor and the host. *Cancer Metastasis Rev.* 27, 691–705 (2008).

70. Salvatierra, E. *et al.* SPARC controls melanoma cell plasticity through Rac1. *PLoS One* (2015). doi:10.1371/journal.pone.0134714

71. Shaverdashvili, K. *et al.* MT1-MMP modulates melanoma cell dissemination and metastasis through activation of MMP2 and RAC1. *Pigment Cell Melanoma Res.* 27, 287–296 (2014).

72. Zhang, X., Yao, X., Qin, C., Luo, P. & Zhang, J. Investigation of the molecular mechanisms underlying metastasis in prostate cancer by gene expression profiling. *Exp. Ther. Med.* 12, 925–932 (2016).

73. Prevarskaya, N., Skryma, R. & Shuba, Y. Calcium in tumour metastasis: New roles for known actors. *Nat. Rev. Cancer* 11, 609–618 (2011).

74. Liu, G., Ren, F. & Song, Y. Upregulation of SPOCK2 inhibits the invasion and migration of prostate cancer cells by regulating the MT1-MMP/MMP2 pathway. *PeerJ* **7**, e7163 (2019).

75. Xia, L. *et al.* Diallyl disulfide inhibits colon cancer metastasis by suppressing Rac1-mediated epithelial-mesenchymal transition . *Onco. Targets. Ther.* (2019). doi:10.2147/ott.s208738

76. Miller, A. J. & Mihm, M. C. mechanisms of disease Melanoma. *new Engl. J. o f Med.* (2006).

77. Cardama, G. A. *et al.* Relevance of small GTPase Rac1 pathway in drug and radio-resistance mechanisms: Opportunities in cancer therapeutics. *Crit. Rev. Oncol. Hematol.* 124, 29–36 (2018).

78. Huelsenbeck, S. C. *et al.* Rac1 protein signaling is required for DNA damage response stimulated by topoisomerase II poisons. *J. Biol. Chem.* 287, 38590–

38599 (2012).

79. Nohata, N. *et al.* Temporal-specific roles of Rac1 during vascular development and retinal angiogenesis. *Dev. Biol.* 411, 183–194 (2016).

80. Hodis, E. *et al.* A landscape of driver mutations in melanoma. *Cell* 150, 251–263 (2012).

81. Song, G. *et al.* Identification of aberrant gene expression during breast ductal carcinoma in situ progression to invasive ductal carcinoma . *J. Int. Med. Res.* 030006051881536 (2019). doi:10.1177/0300060518815364

82. Dunleavey, J. M. *et al.* Vascular channels formed by subpopulations of PECAM1 + melanoma cells. *Nat. Commun.* (2014). doi:10.1038/ncomms6200

83. Lagarrigue, F. *et al.* A RIAM/lamellipodin-talin-integrin complex forms the tip of sticky fingers that guide cell migration. *Nat. Commun.* 6, 1–13 (2015).

84. Liu, W., Peng, Y. & Tobin, D. J. A new 12-gene diagnostic biomarker signature of melanoma revealed by integrated microarray analysis. *PeerJ* 2013, 1–23 (2013).

85. Costantini, F. & Barbieri, G. The HLA-DR mediated signalling increases the migration and invasion of melanoma cells, the expression and lipid raft recruitment of adhesion receptors, PD-L1 and signal transduction proteins. *Cell. Signal.* 36, 189–203 (2017).

86. Kovacs, D. *et al.* The role of Wnt/β-catenin signaling pathway in melanoma epithelial-to-mesenchymal-like switching: Evidences from patients-derived cell lines. *Oncotarget* 7, 43295–43314 (2016).

87. Xie, Y., Li, F., Li, Z. & Shi, Z. miR-135a suppresses migration of gastric cancer cells by targeting TRAF5-mediated NF-κB activation. *Onco. Targets. Ther.* 12, 975–984 (2019).

88. Li, M., Long, C., Yang, G., Luo, Y. & Du, H. MiR-26b inhibits melanoma cell proliferation and enhances apoptosis by suppressing TRAF5-mediated MAPK activation. *Biochem. Biophys. Res. Commun.* 471, 361–367 (2016).

89. Liang, Z. *et al.* MiR-141–3p inhibits cell proliferation, migration and invasion by

targeting TRAF5 in colorectal cancer. *Biochem. Biophys. Res. Commun.* 514, 699–705 (2019).

90. Zhang, L. *et al.* LncRNA KTN1-AS1 promotes tumor growth of hepatocellular carcinoma by targeting miR-23c/ERBB2IP axis. *Biomed. Pharmacother.* 109, 1140–1147 (2019).

91. Gottesdiener, L. S. *et al.* Rates of ErbB2 alterations across melanoma subtypes and a complete response to trastuzumab emtansine in an ErbB2-amplified acral melanoma. *Clin. Cancer Res.* (2018). doi:10.1158/1078-0432.CCR-18-1397

92. Le Coz, V. *et al.* IGF-1 contributes to the expansion of melanoma-initiating cells through an epithelial-mesenchymal transition process. *Oncotarget* **7**, 82511–82527 (2016).

93. Mirmohammadsadegh, A. *et al.* STAT5 phosphorylation in malignant melanoma is important for survival and is mediated through SRC and JAK1 kinases. *J. Invest. Dermatol.* 126, 2272–2280 (2006).

94. Hongu, T. *et al.* Arf6 regulates tumour angiogenesis and growth through HGF-induced endothelial β1 integrin recycling. *Nat. Commun.* 6, (2015).

95. Ruiz, A., Nadal, M., Puig, S. & Estivill, X. Cloning of the human phospholipase A2 activating protein (hPLAP) gene on the chromosome 9p21 melanoma deleted region. *Gene* (1999). doi:10.1016/S0378-1119(99)00354-6

96. Bid, H. K., Roberts, R. D., Manchanda, P. K. & Houghton, P. J. RAC1: An emerging therapeutic option for targeting cancer angiogenesis and metastasis. *Molecular Cancer Therapeutics* (2013). doi:10.1158/1535-7163.MCT-13-0164

97. Tal, O. *et al.* DC mobilization from the skin requires docking to immobilized CCL21 on lymphatic endothelium and intralymphatic crawling. *J. Exp. Med.* 208, 2141–2153 (2011).

98. Bosco, E. E., Mulloy, J. C. & Zheng, Y. Rac1 GTPase: A 'Rac' of all trades. *Cellular and Molecular Life Sciences* (2009). doi:10.1007/s00018-008-8552-x

99. Marei, H. & Malliri, A. Rac1 in human diseases: The therapeutic potential of targeting Rac1 signaling regulatory mechanisms. *Small GTPases* 8, 139–163 (2017).

100. Grimes, J. A. *et al.* Agreement Between Cytology and Histopathology for Regional Lymph Node Metastasis in Dogs With Melanocytic Neoplasms. *Vet. Pathol.* (2017). doi:10.1177/0300985817698209

101. Hall, J. S. *et al.* Exon-array profiling unlocks clinically and biologically relevant gene signatures from formalin-fixed paraffin-embedded tumour samples. *Br. J. Cancer* 104, 971–981 (2011).

102. Fohn, L. E. *et al.* D2-40 lymphatic marker for detecting lymphatic invasion in thin to intermediate thickness melanomas: Association with sentinel lymph node status and prognostic value - A retrospective case study. *J. Am. Acad. Dermatol.* (2011). doi:10.1016/j.jaad.2010.03.005

103. Padera, T. P. *et al.* Lymphatic metastasis in the absence of functional intratumor lymphatics. *Science (80-.).* (2002). doi:10.1126/science.1071420

104. Harris, E. I. *et al.* Lymphovascular invasion in colorectal cancer: An interobserver variability study. *Am. J. Surg. Pathol.* (2008). doi:10.1097/PAS.0b013e3181816083

105. Rakha, E. A. *et al.* Diagnostic concordance of reporting lymphovascular invasion in breast cancer. *J. Clin. Pathol.* (2018). doi:10.1136/jclinpath-2017-204981

106. Beggan, C. *et al.* Pattern of invasion and lymphovascular invasion in squamous cell carcinoma of the floor of the mouth: an interobserver variability study. *Histopathology* (2016). doi:10.1111/his.13014